Journal of Sedimentary Research

Journal of Sedimentary Research, 2012, v. 82, 21–36
Research Article
DOI: 10.2110/jsr.2012.2

DEEP-WATER CHANNEL RUN-OUT LENGTH: INSIGHTS FROM SEAFLOOR GEOMORPHOLOGY

JACOB A. COVAULT,[1] EITAN SHELEF,[2] MILES TRAER,[2] STEPHEN M. HUBBARD,[3] BRIAN W. ROMANS,[4] AND ANDREA FILDANI[5]

[1]*Chevron Energy Technology Company, Clastic Stratigraphy R&D, Houston, Texas 77002, U.S.A.*
[2]*Department of Geological and Environmental Sciences, Stanford University, Stanford, California 94305, U.S.A.*
[3]*Department of Geoscience, University of Calgary, Calgary, Alberta T2N 1N4, Canada*
[4]*Virginia Tech Geosciences, 4044 Derring Hall (0420), Blacksburg, Virginia 24061, U.S.A.*
[5]*Chevron Energy Technology Company, Clastic Stratigraphy R&D, San Ramon, California 94583, U.S.A.*
e-mail: jakecovault@gmail.com

ABSTRACT: The seafloor provides high-resolution, but relatively static, perspectives of submarine sediment-routing systems, which can be employed in the development of predictive models of deep-water stratigraphic sequences. We compare 31 seafloor canyon-and-channel systems from predominantly siliciclastic continental margins and discuss their morphologic variability. The longest canyon-and-channel systems of this study generally correspond with relatively mature, passive continental margins associated with some of the largest deep-sea fans in the world with long-term, voluminous, mud-rich sediment supply. Shorter, lower-relief canyon-and-channel systems generally correspond with immature margins associated with relatively meager, sand-rich or mixed-caliber sediment supply. Seafloor continental-margin relief nonlinearly corresponds with canyon-and-channel-system length, with very high-relief margins exhibiting longer canyon-and-channel systems than predicted by a linear relationship. Nonlinearity in our observations can be accounted for by the increased occurrence and magnitude of submarine mass wasting in higher-relief and correspondingly longer canyon-and-channel systems, limitations of relief imposed by the maximum depths of ocean basins, and sediment-gravity-flow dynamics. These interpretations of controls on canyon-and-channel geomorphology represent extrinsic characteristics of land-to-deep-sea sediment supply and basin or continental-margin framework and intrinsic sediment-gravity-flow dynamics.

We demonstrate that insights into seafloor channel processes, morphologic products, and scaling relationships can be broadly applied to predicting ancient subsurface and outcropping deep-water stratigraphic sequences. Our comparative analysis suggests that knowledge of the thickness of an ancient basin-margin stratigraphic sequence can be employed in order to generally predict the basinward extent of a paleo-canyon-and-channel system and underlying depositional fan. The application also potentially works in reverse: intimate knowledge of the deep-water component of a continental margin or basin margin can facilitate understanding of up-depositional-dip stratigraphic architectures where data might be lacking.

INTRODUCTION

Deep-water depositional systems represent the final resting places of sediment gravity flows along basin-margin routing systems, and ancient deep-water strata are an important focus of oil and gas exploration projects. Since the late twentieth century, sequence-stratigraphic techniques have been employed in order to place deep-water sediment and sedimentary rocks into a predictive chronostratigraphic framework (e.g., Payton 1977; Wilgus et al. 1988; Posamentier et al. 1991; Posamentier and Kolla 2003). In general, sequence-stratigraphic methods enhance predictions of grain-size distribution and reservoir quality of deep-water systems (Fig. 1). However, predictions of the absolute extents of these systems, which range in relief from hundreds to thousands of meters and length from tens to thousands of kilometers, generally are not available, and this information can be of fundamental importance in delineation and subsequent development of hydrocarbon reservoirs (Fig. 1).

Normark (1970) provided one of the first models of modern deep-water depositional systems and their architectures predominantly from seafloor morphologies, which instigated a revolution in marine geology and petroleum-industry research and development of such models. Concerns regarding comparisons of seafloor observations and contemporaneously developing concepts from ancient subsurface and outcropping deep-water systems (e.g., Normark 1978; Walker 1978; Nilsen 1980) prompted investigation of practical common ground between modern and ancient systems, some of the results of which hold true to this day (Bouma et al. 1985; Mutti and Normark 1987; Mutti and Normark 1991; Normark et al. 1993). Subsequent studies of deep-water depositional systems have attempted to rigorously and inclusively quantify their morphologic characteristics in order to enhance predictability (e.g., Wetzel 1993; Reading and Richards 1994; Steffens et al. 2003; Carvajal et al. 2009; Sømme et al. 2009a; Sømme et al. 2009b). These efforts attempted to integrate diverse approaches: i.e., methods typically employed for terrestrial geomorphologic observations, which established relationships between drainage-basin area, river length, and gradient (e.g., Milliman and Syvitski 1992), and conventional deep-water stratigraphic analyses. Here we provide a new contribution to the burgeoning Earth science subdiscipline of seafloor geomorphology, which has only recently been possible as a result of advances in submarine remote-sensing technology.

Published Online: January 2012
 1527-1404/12/082-025/$03.00

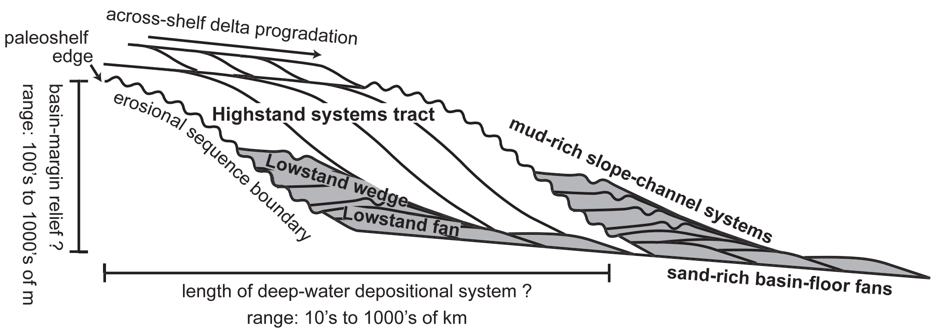

FIG. 1.—Generalized sequence-stratigraphic model of a continental margin. Relatively coarse-grained deep-water systems tracts are shaded. The absolute lengths and reliefs of deep-water depositional systems vary over orders of magnitude between margins.

This technology provides high-resolution three-dimensional seismic-reflection, multibeam bathymetry, and sidescan sonar surveys of continental margins. We present a compilation of seafloor canyon-and-channel metrics, including run-out length, thalweg gradient, and continental-margin relief, for predictions and insights into the spatial distribution of deep-water channels and stratigraphic sequences (Fig. 2). Quantitative morphologic relationships documented herein are applicable to natural-resource exploration in data-poor regions and shed light onto deep-water channel processes fundamental to the understanding of turbidite depositional patterns.

SEAFLOOR CANYON-AND-CHANNEL DATABASE

Our seafloor database includes measurements of length, thalweg gradient, and relief of 31 canyon-and-channel systems (Table 1; Figs. 2, 3, 4). These systems are numbered from 1 to 31 for ease of comparison in figures and Table 1. Throughout the paper, canyon-and-channel names are followed by the corresponding number in parentheses. We attempted to sample canyon-and-channel longitudinal profiles from a global range of continental margins: from the tectonically active transform and convergent margins of the Pacific to the Atlantic passive margin offshore the Americas (Table 1; Fig. 2) (Covault et al. 2011). We examined profiles of canyons and channels that are present across the seafloor (i.e., buried channel features are excluded) and, as such, they represent the most recent canyon-and-channel-system activity (i.e., since the last glacial cycle, < 100 ka, for many systems; Lambeck and Chappell 2001) (Fig. 2) (Covault et al. 2011). These canyon-and-channel systems are submarine conduits that pass from predominantly erosional V-shaped canyons indenting the shelf and uppermost slope to U-shaped channels with overbank deposits across the lower slope and continental rise (cf. Shepard 1948; Menard 1955; Normark 1970; Carter 1988; Covault et al. 2011) (Fig. 2). Canyon-and-channel systems transition to depositional lobe architectures across the channel-to-lobe transition zone (e.g., Normark 1970; Normark et al. 1979; Mutti and Normark 1987; Wynn et al. 2002; Jegou et al. 2008) (Fig. 2). The channel terminus is the point on the seafloor at which a main trunk channel ends and/or breaks into multiple channels (Fig. 2).

We attempted to measure length and relief of 19 canyon-and-channel longitudinal profiles from canyon head to near the point of the channel terminus at the end of the channel-to-lobe transition zone (Figs. 2, 3, 4). Four canyon-and-channel profiles from the California Continental Borderland were measured from NOAA-NGDC and USGS multibeam bathymetry: Newport (10), Oceanside (11), Carlsbad (12), and La Jolla (14) (< 3 arc-second grids, 10-cm vertical resolution; Gardner and Dartnell 2002; Dartnell et al. 2007; Divins and Metzger 2010; Table 1). The remaining profiles were compiled from published examples to facilitate further investigation of the canyons and channels of this study (Table 1). The majority of profiles were measured by other researchers from high-resolution three-dimensional seismic-reflection and multibeam bathymetric data (Table 1). Regardless of the resolution of published longitudinal profiles, long and short profiles are compared at similar resolutions as a result of the following measurement procedure: (1) water depths and down-system lengths were measured along every bend (cf. channel length and slope measurements of Flood and Damuth 1987); and (2) water depths and down-system lengths of the high-resolution profiles were re-sampled every 10 km for systems > 100 km long and every 1 km for systems < 100 km long (Covault et al. 2011). Down-canyon-and-channel gradient was also calculated. Gradient was calculated every 10 km for systems > 100 km long and every 1 km for systems < 100 km long (except for the Norfolk (18) and Washington (19) systems, across which gradient was calculated every 2 km).

A number of longitudinal profiles do not extend from canyon head to channel terminus. The East Breaks (15) channel terminates in an intraslope basin (Pirmez et al. 2000). The Astoria (5), Nigeria X (16), Hudson (17), Norfolk (18), Washington (19), and Laurentian (21) systems were not measured to their channel termini because of limitations of three-dimensional seismic-reflection and bathymetric data coverage (Table 1) (Pirmez et al. 2000). The lengths of these canyon-and-channel systems generally are measured only across continental slopes and, as a result, lengths from canyon head to channel terminus are underestimated. Because the terminal segments of these canyon-and-channel systems extend across relatively low gradients of the lower continental slope and rise, these systems do not extend into much deeper water, and the corresponding relief-to-length ratio of canyon-and-channel systems is probably too low.

Published catalogs of canyon-and-channel metrics were also incorporated for analysis (Wetzel 1993; Reading and Richards 1994; Sømme et al. 2009a) (Table 1). These catalogs include data on system length and relief for an additional 12 systems (Table 1).

CANYON-AND-CHANNEL SYSTEMS

Canyon-and-channel systems are presented according to continental-margin type following the general classification scheme of Bouma et al. (1985) and Barnes and Normark (1985): tectonically active and passive continental margins (Table 1; Figs. 2, 3). Tectonically active margins generally include convergent and California transform margins. Passive margins generally include slopes subjected to gravity-driven tectonic deformation that produces diapirism, growth faults, folds, and toe thrusts, and mature (i.e., long-lived) margins not subjected to appreciable tectonic uplift, but gradual subsidence as a result of thermal cooling of the lithosphere (Carter 1988). Mature margins can be associated with some of the largest deep-sea fans in the world with long-term, voluminous sediment supply (Barnes and Normark 1985).

Tectonically Active Continental Margins

The Barbados A (1), San Antonio (2), Kushiro (3), Aoga (4), Astoria (5), and Nitinat (6) canyon-and-channel systems are from tectonically active convergent margins subjected to synsedimentary tectonic deformation (Table 1; Figs. 2, 3). The Barbados A (1), San Antonio (2),

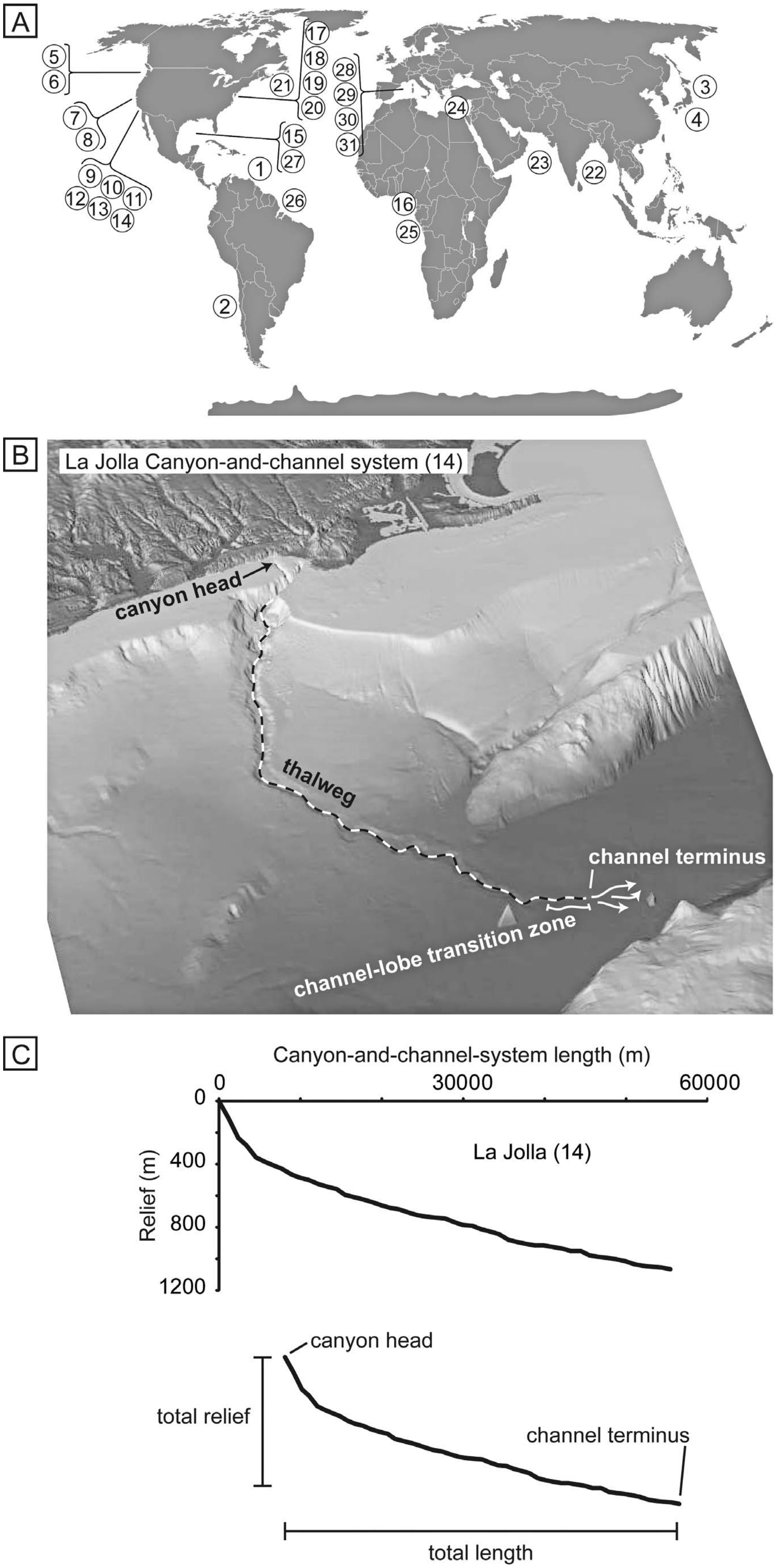

FIG. 2.—**A)** Seafloor systems used in this study. Numbers correspond to systems in Table 1. **B)** Bathymetric image of the La Jolla Canyon-and-channel system offshore southern California. Canyon head, canyon-and-channel thalweg, channel-lobe transition zone, and channel terminus are identified. Bathymetry and onshore topography from GeoMapApp http://www.geomapapp.org (Ryan et al. 2009). **C)** Longitudinal profile along the La Jolla Canyon-and-channel thalweg, with canyon head, and channel terminus identified for reference.

TABLE 1.—*Characteristics of canyon-and-channel systems.*

System	(1)Barbados A	(2)San Antonio	(3)Kushiro	(4)Aoga	(5)Astoria	(6)Nitinat	(7)Delgada	(8)Monterey	(9)Hueneme	(10)Newport
Geographic context	Venezuela, Caribbean Sea	central Chile, Pacific Ocean	Hokkaido, Japan, Pacific Ocean	Honshu, Japan, Pacific Ocean	Washington, USA, Pacific Ocean	Washington, USA, Pacific Ocean	northern California, USA, Pacific Ocean	central California, USA, Pacific Ocean	southern California, USA, Pacific Ocean	southern California, USA, Pacific Ocean
Bathymetry data	200-m-resolution digital elevation models with a vertical accuracy of 0.6% of depth	Hydrosweep bathymetry (better than 100-m horizontal resolution)	SeaBeam and Hydrosweep bathymetry (measured over 5 km)	1980s-vintage SeaMARC II bathymetry (measured over < 10 km)	1960s-vintage bathymetry (measured over < 10 km)	N/A	N/A	N/A	N/A	NOAA/NGDC/USGS bathymetry (< 3 arc-second grids; 10-cm vertical resolution)
Margin type	Active, convergent	Active, convergent	Active, convergent	Active, convergent	Active, convergent	Active, convergent	Active, transform	Active, transform	Active, transform	Active, transform
Synsed. deformation	Yes	Yes	Yes	Yes	Yes	Yes	Yes	Yes	Yes	Yes
Dep. sys. age	Quaternary	Quaternary	since Neogene	since Neogene	Quaternary	Quaternary	since Miocene	since Miocene	Quaternary	Quaternary
Measured length (km)	250	110	200	200	240	260	350	400	50	110
Measured relief (m)	2020	4460	6370	5760	2790	2800	4300	4700	900	1060
Fluvial sediment load ($\times 10^6$ t / yr)	N/A†	3.2 km^3 / yr§	10 km^3 / yr#	N/A†	15	20	1.5	4.8	3.8	0.5
Grain size	mud to gravel	mud to coarse-grained sand	mud to pebbles	presumably mud to pebbles	mud to gravel; silt rich	mud to coarse-grained sand; silt rich	mud to sand; mud rich	mud to cobbles; mud rich	mud to coarse-grained sand; sand rich	mud to gravel; sand rich
References	14	19,21	24	17	2,22,31,35,39,40	2,18,35,39,40	2,26,31,35, 39,40	2,13,31,35, 39,40	29,30,31,36,39	12,16,30

System	(11)Oceanside	(12)Carlsbad	(13)Navy	(14)La Jolla	(15)East Breaks	(16)Nigeria X	(17)Hudson	(18)Norfolk	(19)Washington	(20)Wilmington
Geographic context	southern California, USA, Pacific Ocean	southern California, USA, Pacific Ocean	southern California, USA, Pacific Ocean	southern California, USA, Pacific Ocean	NW Gulf of Mexico	Niger Delta, Atlantic Ocean	New Jersey, USA, Atlantic Ocean	Virginia, USA, Atlantic Ocean	Virginia, USA, Atlantic Ocean	Maryland-Delaware, USA, Atlantic Ocean
Bathymetry data	NOAA/NGDC/USGS bathymetry (< 3 arc-second grids; 10-cm vertical resolution)	NOAA/NGDC/USGS bathymetry (< 3 arc-second grids; 10-cm vertical resolution)	N/A	NOAA/NGDC/USGS bathymetry (< 3 arc-second grids; 10-cm vertical resolution)	3D seismic-reflection data (processed bin size of 50 × 25 m)	3D seismic-reflection data	SeaBeam bathymetry (measured over 5 km)	Information not provided	Information not provided	N/A
Margin type	Active, transform	Active, transform	Active, transform	Active, transform	Passive	Passive	Passive	Passive	Passive	Passive
Synsed. deformation	Yes	Yes	Yes	Yes	Yes; gravity-driven	Yes; gravity-driven	No	No	No	No
Dep. sys. age	Quaternary	Quaternary	Quaternary	Quaternary	Quaternary	Quaternary	since Neogene	since Neogene	since Neogene	since Neogene
Measured length (km)	60	30	40	50	60	80	270	90	100	600

TABLE 1.—*Continued.*

System	(11)Oceanside	(12)Carlsbad	(13)Navy	(14)La Jolla	(15)East Breaks	(16)Nigeria X	(17)Hudson	(18)Norfolk	(19)Washington	(20)Wilmington
Measured relief (m)	960	680	1900	1040	1020	1420	3900	2280	2490	4600
Fluvial sediment load (× 10^6 t / yr)	0.4	unknown, but likely small	0.21	2.2 (Oceanside littoral cell)	16	40	1	unknown, but likely small	unknown, but likely small	1
Grain size	mud to gravel; sand rich	mud to gravel; sand rich	mud to gravel; sand rich	mud to gravel; sand rich	mud to sand	mud to sand	mud to gravel; mud rich	mud to sand; mud rich	mud to sand; mud rich	mud to sand; mud rich
References	7,12,16,30	7,30	2,27,30,40	7,12,15,25,30,35	3,4,20,33	20,33	5,20,34	6,11	6,11	6,35,39

System	(21)Laurentian	(22)Bengal	(23)Indus	(24)Nile	(25)Zaire	(26)Amazon	(27)Mississippi	(28)Ebro	(29)Rhone	(30)Golo	(31)Var
Geographic context	eastern Canada, Atlantic Ocean	Bay of Bengal	Arabian Sea	Egypt, Mediterranean Sea	West Africa, Atlantic Ocean	Brazil, Atlantic Ocean	Gulf of Mexico	Spain, Mediter-ranean Sea	France, Mediter-ranean Sea	Corsica, Mediter-ranean Sea	France, Mediter-ranean Sea
Bathymetry data	1980s-vintage SeaBeam bathymetry	N/A	N/A	N/A	Simrad bathymetry (better than 100-m horizontal resolution; 10-m vertical resolution)	SeaBeam bathymetry (~ 100-m horizontal resolution)	N/A	N/A	1980s-vintage SeaBeam and SeaMARC I bathymetry	N/A	Information not provided
Margin type	Passive	Mixed*	Mixed*	Passive	Passive	Passive	Passive	Mixed*	Mixed*	Mixed*	Mixed*
Synsed. deformation	No	No	No	No	Yes; gravity-driven	No	Yes; gravity-driven	No	No	Yes	Yes; Qt. terrace uplift, earthquakes common
Dep. sys. age	Quaternary	since Eocene	since Oligocene	since Miocene	since Oligocene	since Miocene	since Pliocene	Quaternary	since Pliocene	Quaternary	since Pliocene
Measured length (km)	360	3000	1500	280	1030	800	540	50	170	20	140
Measured relief (m)	4270	5000	4600	3000	4820	4050	3300	1800	2090	700	2470
Fluvial sediment load (× 10^6 t / yr)	4	980	450	240	48	1200	400	20	7.4	0.71	1.3
Grain size	mud to gravel; sand rich	mud to sand; mud rich	mud to sand; mud rich	mud to sand; mud rich	mud rich	mud to pebbles; mud rich	mud rich	mud to medium-grained sand; sand rich	mud to fine-grained sand; silt rich	mud to gravel; sand rich	sand rich
References	2,20,35,38,40	2,8,35,39,40	2,35,39,40	2,35,39,40	1,39,40	2,10,32,31, 33,35,39,40	2,31,35,39,40	2,23,35,39,40	2,28,33, 35,39,40	9,39	37,39

* Mixed margins include settings adjacent to uplifting hinterland source areas (e.g., the Bay of Bengal, Arabian Sea, and the Mediterranean Sea). The northwestern Mediterranean Sea is a young, steep margin (post Oligocene) with local tectonism (Savoye et al. 1992).

† These canyons head on the middle continental slope, rather than the shelf edge.

§ Rio Miapo discharge (not fluvial sediment load).

Combined discharge of the Tokachi and Kushiro rivers (not fluvial sediment load).

References: (1) Babonneau et al. (2002); (2) Barnes and Normark (1985); (3) Beaubouef and Friedmann (2000); (4) Booth et al. (2000); (5) Butman et al. (2006); (6) Cleary et al. (1985); (7) Covault et al. (2007); (8) Curray et al. (2002); (9) Deptuck et al. (2008); (10) Flood et al. (1991); (11) Gerber et al. (2009); (12) Graham and Bachman (1983); (13) Greene et al. (2002); (14) Huyghe et al. (2004); (15) Inman (2008); (16) Inman and Jenkins (1999); (17) Klaus and Taylor (1991); (18) Knudson and Hendy (2009); (19) Laursen and Normark (2002); (20) Milliman and Syvitski (1992); (21) Milliman et al. (1995); (22) Nelson (1970); (23) Nelson et al. (1985); (24) Noda et al. (2008); (25) Normark (1970); (26) Normark and Gutmacher (1985); (27) Normark and Piper (1985); (28) Normark et al. (1985); (29) Normark et al. (2006); (30) Normark et al. (2009); (31) Piper and Normark (2001); (32) Pirmez and Imran (2003); (33) Pirmez et al. (2000); (34) Pratson et al. (1994); (35) Reading and Richards (1994); (36) Romans et al. (2009b); (37) Savoye et al. (1993); (38) Skene and Piper (2006); (39) Sømme et al. (2009a); (40) Wetzel (1993).

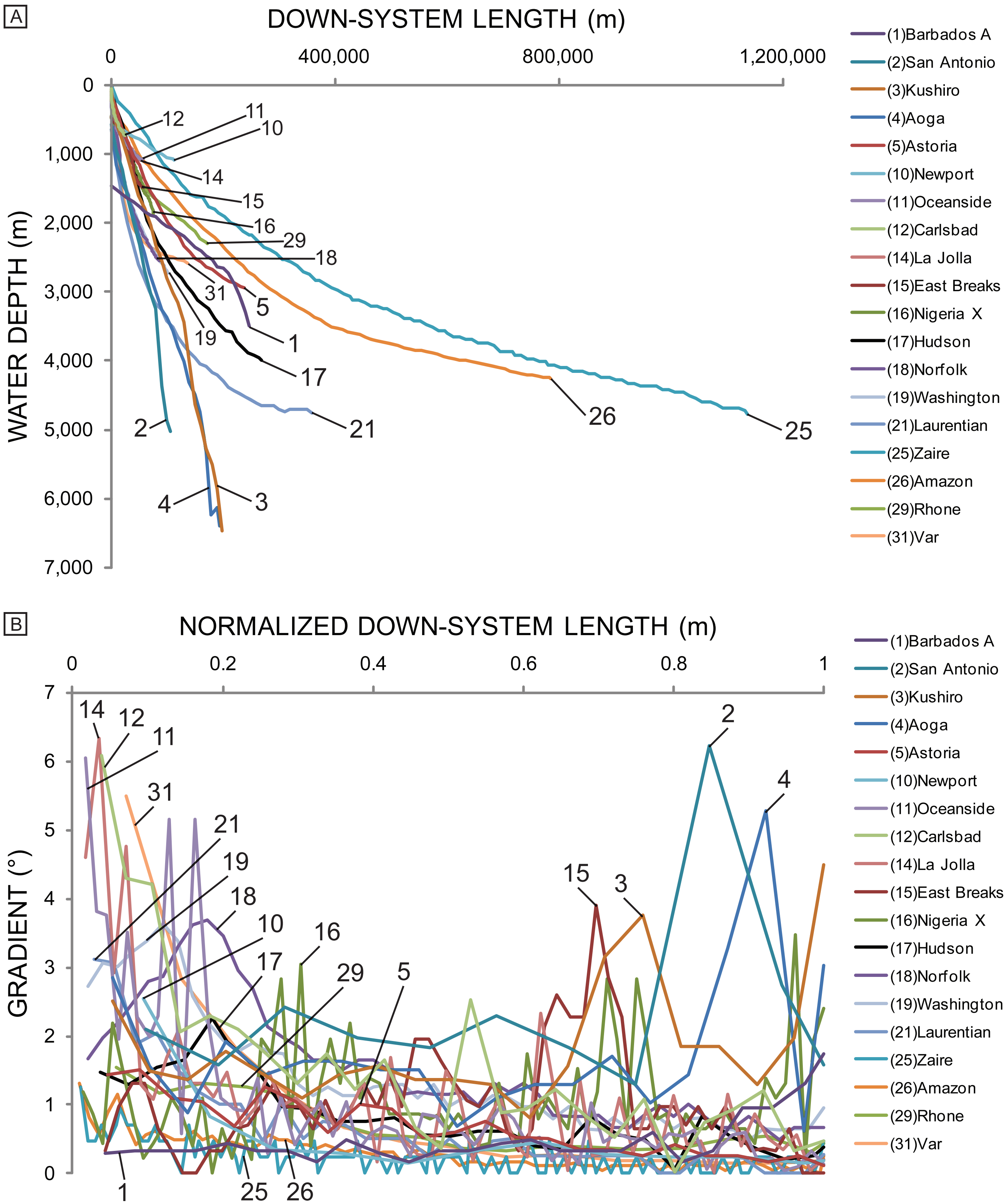

FIG. 3.—**A)** Seafloor canyon-and-channel longitudinal profiles. **B)** Seafloor canyon-and-channel thalweg gradients across normalized lengths. Numbers correspond to systems in Table 1.

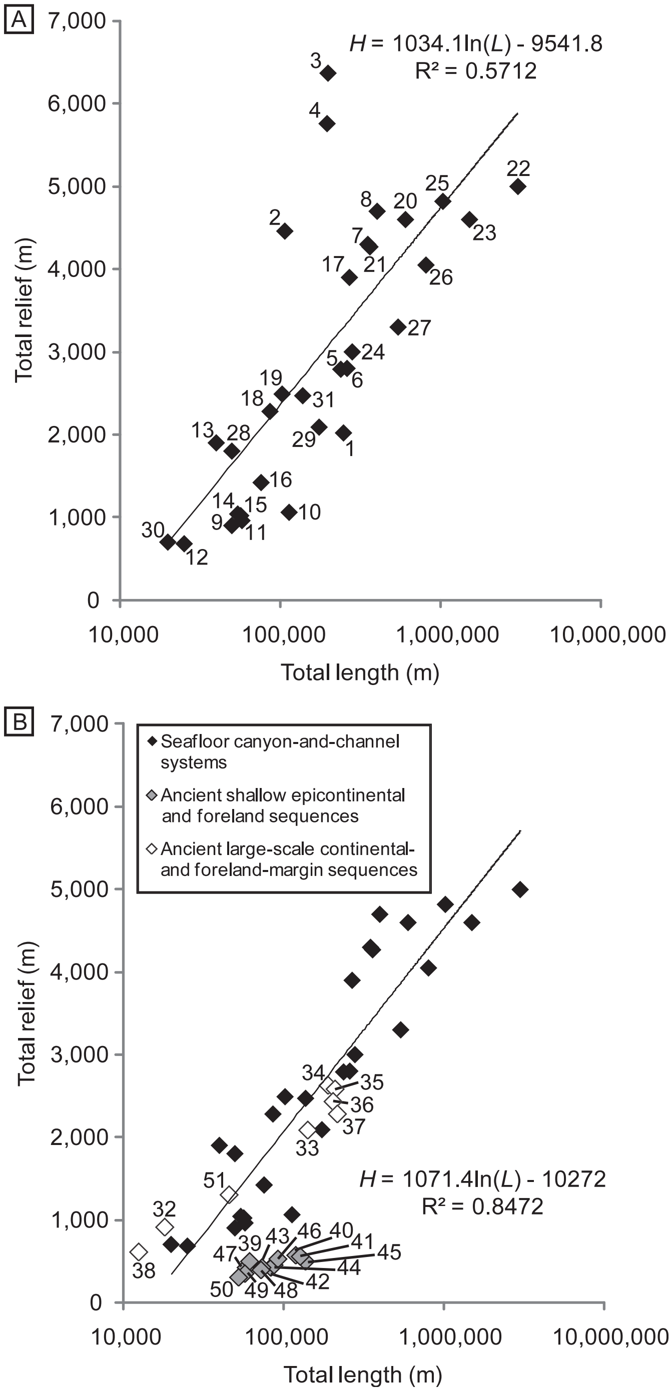

FIG. 4.—**A)** Relief versus length of seafloor canyon-and-channel systems. Numbers correspond to systems in Table 1. **B)** Relief versus length of seafloor canyon-and-channel systems except the San Antonio (2), Kushiro (3), and Aoga (4) systems. Ancient subsurface and outcropping paleo–shelf–slope–basin-floor sequences are also included (Table 2). Only seafloor data (black diamonds) were used in determining the correlation function.

Kushiro (3), and Aoga (4) systems received relatively small volumes of sediment over the last glacial cycle relative to large, mature (i.e., long-lived) submarine fan systems that were provided voluminous sediment in open ocean basins (cf. measurements of fluvial sediment load in Table 1). The San Antonio (2) system offshore Chile and the Kushiro (3) and Aoga (4) systems offshore Hokkaido and Honshu, respectively, are canyon-to-erosional-channel systems that deposited relatively coarse-grained sediment in accretionary wedge-top and forearc basins, and transported sediment across the steep front of accretionary wedges that extend seaward into trenches (Klaus and Taylor 1991; Laursen and Normark 2002; Noda et al. 2008). The Barbados A (1) system offshore Venezuela transported relatively coarse-grained sediment across the Barbados Ridge Complex (Huyghe et al. 2004) (Table 1). The system originates on a tectonically quiescent segment of the continental slope, where the gradient is flatter, which facilitated the development of levee and overbank relief. Across more distal reaches, however, the system lacks levee relief and is incised into the steeper, actively uplifting front of the Barbados Ridge Complex (Huyghe et al. 2004).

The Astoria (5) and Nitinat (6) systems developed across the Cascadia tectonically active convergent margin offshore western North America (Nelson et al. 1970; Zuffa et al. 2000; Knudson and Hendy 2009) (Table 1; Figs. 2, 3). The Cascadia continental shelf and slope are part of a forearc basin and accretionary prism in which the Juan de Fuca plate is being subducting beneath the North American plate (Underwood et al. 2005). Terrigenous sediment dispersal through the Astoria (5) and Nitinat (6) canyon-and-channel systems is highly dependent on climatic fluctuations: the Astoria (5) system was fed relatively large volumes of coarse-grained sediment during subglacial transitions (Brunner et al. 1999; Zuffa et al. 2000; Piper and Normark 2009), whereas sediment supply to the Nitinat (6) system has been linked to ice-sheet extent and transport of glacio-marine sediment across the continental margin (Knudson and Hendy 2009).

The Delgada (7), Monterey (8), Hueneme (9), Newport (10), Oceanside (11), Carlsbad (12), Navy (13), and La Jolla (14) canyon-and-channel systems developed across the California transform continental margin and generally include a mix of sand and mud sediment loads (Normark and Gutmacher 1985; Normark et al. 1985; Piper and Normark 2001; Greene et al. 2002; Fildani and Normark 2004; Normark et al. 2006; Normark et al. 2009) (Table 1; Figs. 2, 3). The Delgada (7) and Monterey (8) systems are not associated with large delta or river systems but appear to receive sediment from shelf-edge canyons that feed sediment to relatively large deep-sea fans (Barnes and Normark 1985; Piper and Normark 2001; Fildani and Normark 2004). These large systems exhibit prominent channel-and-levee complexes (Piper and Normark 2001). The Hueneme (9), Newport (10), Oceanside (11), Carlsbad (12), and Navy (13) canyon-and-channel systems are smaller and developed in confined basins of the California Continental Borderland (Normark et al. 2009). They developed across relatively steep, tectonically active slopes outboard of narrow shelves and nearby hinterlands from which relatively coarse-grained sediment is shed (Normark et al. 2006; Normark et al. 2009). These systems are fed by mixed-sediment-caliber river deltas and, as a result, are sensitive to climatic changes in the hinterland (Piper and Normark 2001; Romans et al. 2009; Covault et al. 2010). The La Jolla (14) system also developed in the California Borderland. It includes a canyon that transitions to a channel with modest levee and overbank relief and terminates as depositional lobes. This system lacks a prominent contributor of fluvial sediment, however, its canyon head has been incised across the continental shelf to the modern beach, where it intercepts littoral-drift-transported sand (Covault et al. 2007).

Passive Continental Margins

The East Breaks (15), also known as the Brazos–Trinity system (e.g., Mallarino et al. 2006), and Nigeria X (16) canyon-and-channel systems are from passive continental margin slopes subjected to gravity-driven tectonic deformation that produces diapirism, growth faults, folds, and toe thrusts (e.g., the intraslope basin province of the northwestern Gulf of Mexico for East Breaks (15) and offshore the Niger Delta continental margin for Nigeria X (16); Damuth 1994; Rowan et al. 2004) (Table 1;

Figs. 2, 3). They were subjected to synsedimentary tectonic deformation and received relatively small volumes of sediment over the last glacial cycle relative to large, mature (i.e., long-lived) submarine fan systems that were provided voluminous sediment in open ocean basins (cf. depositional system ages and fluvial sediment load measurements in Table 1). The development of depositional architecture on passive margins deformed by gravity-driven processes (East Breaks (15) and Nigeria X (16)) corresponds with subtle gradient changes across their diapiric and growth-faulted slopes (Prather et al. 1998; Pirmez et al. 2000). Relatively fine-grained, shelf-edge-delta-fed sediment was transported through leveed channels of the East Breaks (15) and Nigeria X (16) slope channels to pockets of intraslope accommodation, where ponded turbidite systems developed (Beaubouef and Friedmann 2000; Booth et al. 2000; Pirmez et al. 2000).

The Hudson (17), Norfolk (18), Washington (19), and Wilmington (20) canyon-and-channel systems developed across the Atlantic passive continental margin offshore the eastern USA, which exhibits steeper regional and local slopes relative to mature margins associated with large deep-sea fans and long-term, voluminous sediment supply (Pratson and Haxby 1996) (Table 1; Figs. 2, 3). These canyon-and-channel systems were predominantly supplied mixed-caliber sediment, from mud to gravel (Pratson et al. 1994; Butman et al. 2006), during periods of lowered sea level, when glacial outwash streams incised the shelf and icebergs even scraped the surface (Duncan and Goff 2001; Fulthorpe and Austin 2004). Progradational clinothem architectures appear to have built out the continental slope and rise (e.g., the Hudson Apron; Greenlee et al. 1992), which are incised by erosional gullies and channels that generally coalesce to disperse sediment across the Wilmington deep-sea fan and Hatteras abyssal plain (Cleary et al. 1985; Schlee and Robb 1991; Pratson et al. 1994). The Laurentian (21) canyon-and-channel system developed across the Atlantic passive margin offshore eastern Canada and, similar to the Astoria (5) system described above, was fed relatively large volumes of coarse-grained sediment during subglacial transitions (Skene and Piper 2006; Piper et al. 2007; Piper and Normark 2009) (Table 1). The Laurentian (13) conduit is remarkable for its straightness, 25-km width, residual buttes, flat erosional floor, and spillover channels (Piper and Normark 2009).

The Bengal (22), Indus (23), Nile (24), Zaire (25), Amazon (26), and Mississippi (27) canyon-and-channel systems are associated with some of the largest deep-sea fans in the world with long-term, voluminous sediment supply (Barnes and Normark 1985) (Table 1; Figs. 2, 3). These generally mud-rich systems include enormous canyons that transition to channels with well-developed levee and overbank relief and terminate as depositional lobes in some cases greater than one thousand kilometers down system in open ocean basins (e.g., Jegou et al. 2008). Even though Barnes and Normark (1985) identify the Bengal (22) and Indus (23) canyon-and-fan systems as having developed on a passive margin, their Oligo-Miocene initiation was a direct result of India–Asia collision and consequent uplift of the Himalayas and the Tibetan Plateau (Curray et al. 2002). Moreover, uplift of the Himalayas has been linked to South Asian summer monsoonal intensity that facilitated voluminous sediment supply to the Bengal (22) and Indus (23) canyon heads (Clift et al. 2008).

The Ebro (28), Rhone (29), Golo (30), and Var (31) canyon-and-channel systems developed in the Mediterranean Sea, which has been interpreted to include passive continental margins (e.g., Barnes and Normark 1985) and/or mixed continental margins (e.g., Sømme et al. 2009a) because they share many of the characteristics of tectonically active margins (Table 1; Figs. 2, 3). That is, the Mediterranean margins are characterized by relatively steep slopes outboard of narrow shelves and uplifting hinterlands from which relatively coarse-grained sediment is shed. However, there are significant differences among Mediterranean systems. Pratson et al. (1994) related the Ebro (28) system to those of the Atlantic passive margin offshore the eastern U.S.A., in which lateral shifts of shelf-edge delta depocenters facilitated the development of multiple channels and gullies across the continental slope, some of which coalesce across the rise. Piper and Normark (2001) likened the Rhone (29) to a large, mature, mud-rich passive-margin canyon-and-channel system similar to the Bengal (22), Indus (23), Nile (24), Zaire (25), Amazon (26), and Mississippi (27) systems. Piper and Normark (2001) likened the Golo (30) and Var (31) to smaller, mixed-sediment-caliber systems in which sediment supply is sensitive to climate changes in the nearby hinterland, similar to the Hueneme (9), Newport (10), Oceanside (11), Carlsbad (12), and Navy (13) systems (Deptuck et al. 2008; Sømme et al. 2009a; Sømme et al. 2011).

Continental-Margin Relief and Canyon-and-Channel Length

The breadth of canyon-and-channel systems analyzed in this study includes short ($<$ 100 km) and long ($>$ 1000 km) systems with relief between $<$ 700 and $>$ 6000 m (Table 1; Figs. 3, 4). Figure 4A shows a plot of total length versus relief for all 31 canyon-and-channel systems. The data generally are positively related according to a logarithmic function of the form

$$H = 1034.1 \ln L\text{-}9541.8 \tag{1}$$

where H is relief, L is length, and ln is the natural logarithm. A logarithmic function indicates that our compilation of canyon-and-channel systems changes quickly and then levels out as systems become longer than ~ 500 km (Fig. 4). Three systems, San Antonio (2), Kushiro (3), and Aoga (4), which developed across tectonically active convergent margins, have greater reliefs for their lengths relative to the other systems (Fig. 4A). When these three systems are removed, the coefficient of determination (r^2 value) from least-squares regression of the relief-to-length relationship is larger, and the data are related according to a logarithmic function of the form (Fig. 4B)

$$H = 1071.4 \ln L - 10272. \tag{2}$$

CONTROLS ON CANYON-AND-CHANNEL RUN-OUT LENGTH

Canyon-and-channel run-out length is discussed relative to tectonic framework and sediment supply. We then discuss the nonlinear relationship between continental-margin relief and canyon-and-channel run-out length in the context of simplified sediment-gravity-flow dynamics. Hypotheses of extrinsic and intrinsic controls on canyon-and-channel run-out are further evaluated with observations of ancient stratigraphic sequences.

Tectonic Setting and Sediment Supply

Generally, the longest canyon-and-channel systems of this study correspond with relatively mature, passive continental margins associated with some of the largest deep-sea fans in the world with long-term, voluminous, mud-rich sediment supply (e.g., the Bengal (22), Indus (23), Nile (24), Zaire (25), Amazon (26), and Mississippi (27) systems; Table 1; Figs. 2, 4, 5A). These canyon-and-channel systems and their underlying depositional fans developed in relatively unconfined, open ocean basins (i.e., type A basins of Mutti and Normark 1987; Barnes and Normark 1985) and, as a result, grew to be relatively extensive (this interpretation was highlighted in works by Nelson and Kulm 1973; Pickering 1982; Kolla and Coumes 1987; Normark 1985; Stow et al. 1985; Mutti and Normark 1987; Kolla and Macurda 1988; Shanmugam and Moiola 1988; Wetzel 1993; Apps et al. 1994; Reading and Richards 1994; Prather et al. 1998; Booth et al. 2000; Piper and Normark 2001; Fildani and Normark 2004; and Covault and Romans 2009; to name a few). Relatively fine

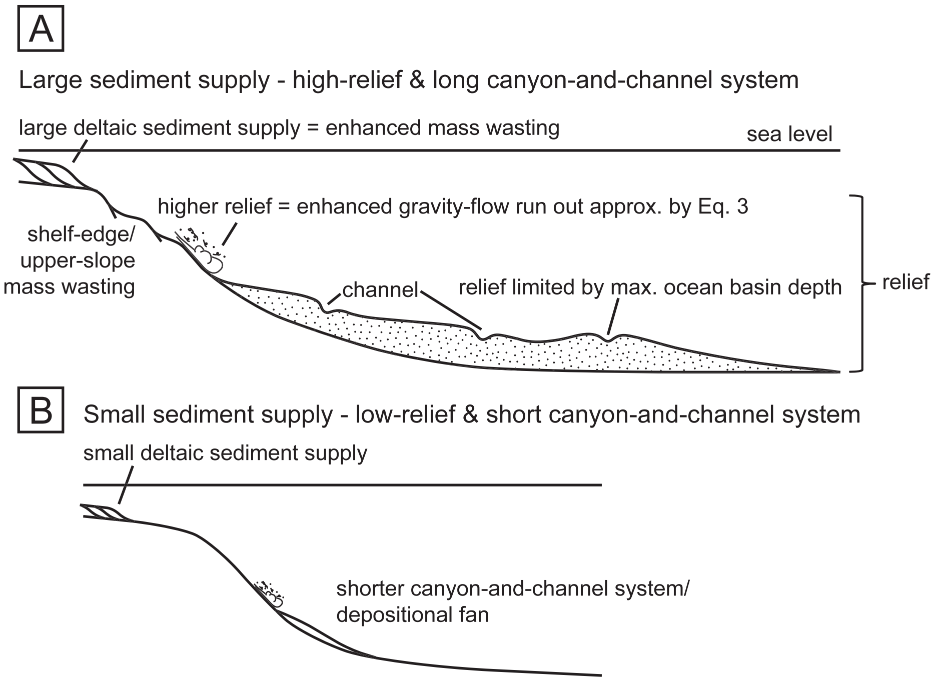

FIG. 5.—End-member canyon-and-channel examples and developmental controls. **A)** Large sediment supply, high-relief, long canyon-and-channel system. **B)** Small sediment supply, lower-relief, shorter canyon-and-channel system.

sediment caliber also contributes to canyon-and-channel system growth (Nelson and Kulm 1973; Stow et al. 1985; Mutti 1992; Wetzel 1993; Reading and Richards 1994). The large, unconfined canyons and fans received predominantly finer-grained sediment, which facilitates sediment-gravity-flow run-out distance (i.e., efficient flows; Mutti 1992) and the development of extensive leveed channel systems across low-gradient, areally extensive fans of the continental rise (Nelson and Kulm 1973; Stow et al. 1985; Mutti 1992; Wetzel 1993; Reading and Richards 1994). These systems also exhibit relatively large relief from canyon head to channel terminus because they extend across continental margins into relatively deep water.

Figure 6 shows that higher-relief continental margins and longer canyon-and-channel systems correspond with larger terrestrial watersheds, which Milliman and Syvitski (1992) linked to larger fluvio-deltaic sediment contributions to the ocean (data also from Sømme et al. 2009a). The reason fluvio-deltaic sediment supply, canyon-and-channel length, and relief are related is that appreciable fluvio-deltaic sedimentation likely promotes the initiation of larger gravity flows and longer durations of canyon-and-channel sediment transfer across margins and into deeper water (Booth et al. 1993; Wetzel 1993; Burgess and Hovius 1998; McAdoo et al. 2000; Carvajal et al. 2009), thereby increasing length and relief over time (Fig. 5A). This progressive extension of canyon-and-channel systems across continental margins and into deeper water is also a contributor to nonlinearity in the relationship of relief to length. That is, submarine canyon-and-channel systems that receive voluminous sediment during a sufficiently long period can only achieve a relief limited by the maximum depth of the ocean basin, but they can extend for great distances (e.g., the Bengal (22) and Indus (23) systems fed voluminous sediment during millions of years from Himalayan sediment source areas; Table 1; Fig. 5A). In this way, canyon-and-channel systems are relief limited; thus, length is a function of relief and not the other way around. Rather, the maximum relief of a continental margin is set by the tectonic framework.

The San Antonio (2), Kushiro (3), and Aoga (4) systems, which developed across tectonically active convergent margins, have much greater reliefs for their lengths relative to the other systems (Fig. 4A). This is a result of their development across relatively steep, high-relief slopes that descend into deep trenches (e.g., Soh and Tokuyama 2002; Ranero et al. 2006; Noda et al. 2008; von Huene et al. 2009). In convergent margins, tectonic processes including basin-localized subsidence, fault-supported inner and outer margin uplift (e.g., Melnick et al. 2006; Collot et al. 2008), and construction of a frontal prism of accreted sediment (Dahlen et al. 1984; Rowan et al. 2004) can steepen the lower slope (Ranero et al. 2006; von Huene et al. 2009). In particular, time-transgressive landward migration of the trench (e.g., Soh and Tokuyama 2002; Noda et al. 2008) and truncation of the submerged forearc caused by frontal subduction erosion can increase slope gradients at the expense of shelf-and-slope seaward extent in convergent settings (Ranero et al. 2006; von Huene et al. 2009).

Shorter, lower-relief canyon-and-channel systems generally correspond with immature margins associated with relatively meager, sand-rich or mixed-caliber sediment supply (e.g., the Hueneme (9), Newport (10), Oceanside (11), Carlsbad (12), Navy (13), La Jolla (14), East Breaks (15), Nigeria X (16), Ebro (28), Golo (30), and Var (31) systems; Table 1; Figs. 2, 4, 5B). These systems generally form on continental-to-transitional crust where continuing tectonic activity resulted in relatively rapid changes in basin morphology and in short-lived sediment sources (i.e., type D basins of Mutti and Normark 1987; e.g., the California Continental Borderland). In such settings, even if canyon-and-channel systems distribute a relatively large volume of sediment, canyon-and-channel extension is limited by basin margins (cf. Covault and Romans 2009). Consequently, corresponding depositional systems tend to be relatively thick compared to their areal extents (cf. turbidite-system growth patterns in the California Continental Borderland; Gorsline and Emery 1959; Covault and Romans 2009). Accommodation renewal in northwestern Gulf of Mexico intraslope basins, and analogous continental margins, occurs as a result of subsidence related to sediment loading and salt and/or mud withdrawal (e.g., the East Breaks (15) and Nigeria X (16) systems; Pratson and Ryan 1994; Prather et al. 1998; Booth et al. 2000; Twichell et al. 2000). Turbidity-current transport and deposition from canyon-and-channel systems can overwhelm the rate of subsidence related to salt tectonics and, as a result, basins are filled with turbidites (Booth et al. 2000). During periods of reduced sediment supply, the rate of basin subsidence, which is driven by the load of the previously

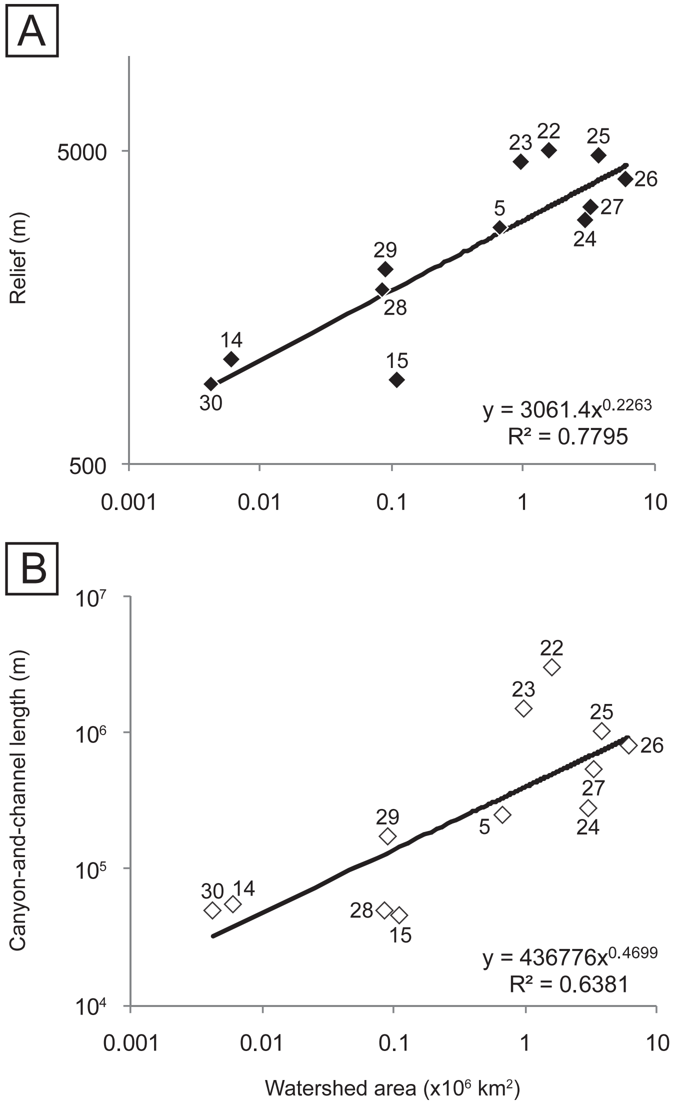

FIG. 6.—Watershed area from Milliman and Syvitski (1992) and Sømme et al. (2009a) versus **A)** continental-margin relief and **B)** canyon-and-channel length.

deposited turbidites, exceeds the rate of deposition and, as a result, accommodation is renewed in basins (Booth et al. 2000; see fig. 10 of Twichell et al. 2000). This process of accommodation renewal is distinctively different from deformation-induced subsidence in the California Continental Borderland. Borderland basins deform primarily as a result of lithospheric plate movements and are more resistant to slight, short-term sediment loading (i.e., turbidite-system growth) relative to gravity-driven passive-margin settings (Rowan et al. 2004). Thus, canyon-and-channel systems with short-lived, sand-rich sediment sources that form in relatively confined basins, some of which are subjected to rapid subsidence related to gravity-driven tectonic deformation, appear to develop length and relief that are distinctively different than in longer-lived, finer-grained systems in large, unconfined ocean basins (Mutti and Normark 1987).

Sediment-Gravity-Flow Dynamics

The positive correlation between continental-margin relief (measured from proximal canyon heads to distal channel termini) and canyon-and-channel length is intuitive because sediment gravity flows that initiate near the top of a higher-relief margin have larger gravitational potential energy and, as a consequence, a longer run-out distance is required for frictional dissipation of the related kinetic energy (Fig. 4). Assuming a block model of flow in which potential energy is balanced entirely by downstream expenditure of flow energy through friction, we would predict a linear relationship between margin relief and canyon-and-channel length. However, the logarithmic relationship exhibited in Figure 4 (Equations 1 and 2) shows that very high-relief margins have longer canyon-and-channel systems than predicted by a linear relationship. This begs the question: how might we account for nonlinearity in our observations?

We developed a scaling argument using depth-averaged theory of a highly simplified sediment gravity flow to address the possible influence of gravity-flow dynamics on nonlinear canyon-and-channel run-out. A complete derivation, as well as complete descriptions of all assumptions made, can be found in the Appendix to this paper. For simplicity, we assume that flows are uniform and steady. Expanding and rearranging the momentum budget, we find that slope (S):

$$S = \Lambda \big/ \left(hU^3\right) \tag{3}$$

where $\Lambda = [r_0\, v_s^{\,5}(c_D+e_w)]/(Fc_D^{\,5/2}RgR_p^{\,3})$ and Λ is a constant arising from our assumption that grain size and ratio of near-bed to depth-averaged concentration are constant values (see Parker et al. 1986; for discussion of these assumptions). The variables of note are the flow height (h) and flow velocity (U) in Equation 3. All other variables are defined in the Appendix to this paper.

Defining slope as margin relief divided by canyon-and-channel run-out distance, analysis of Equation 3 shows that if margin relief is increased (analogous to an increase in S), then run-out distance must correlate with nonlinear changes in flow dynamics (RHS of Equation 3). As these flow dynamics ultimately control the run-out length of an individual flow, and these flows produce the morphologies measured and presented herein, their nonlinear reactions to changes in relief would likewise lead to nonlinear changes in run-out distance. We acknowledge a number of oversimplifying assumptions made for sediment gravity flow in this scaling argument. Among the more severe assumptions, we assert that flows are steady and uniform, coefficient of bed roughness is independent of flow conditions, the Richardson number is slope dependent, and downstream pressure changes resulting from changing flow concentration and height do not significantly affect flow momentum. However, this exercise can be followed using the full momentum budget (Equation A1 in Appendix) to show that any added complexities would only add to the nonlinear compensation of flow dynamics to changes in system relief (cf. Traer et al. in press).

Mitchell (2006) developed simple numerical models of seafloor erosion that are analogous to detachment- and transport-limited erosion models of fluvial geomorphology. In the context of submarine environments, detachment-limited models generally assume that sediment gravity flows can transport an infinite amount of sediment, and erosion of the seafloor is related to the flow shear stress (cf. Howard 1994), which is partly related to seafloor gradient (i.e., if flow parameters such as thickness and density are held constant; Mitchell 2006). In transport-limited models (e.g., Tucker and Whipple 2002), sediment gravity flows are limited in the amount of sediment they can transport by the transporting capacity of the flow, but material is easily detached from the seafloor (Mitchell 2006). That is, all available energy in sediment gravity flows is applied to suspending and transporting sediment, which leads to diffusive-like, smoothing bed changes partly related to the canyon-and-channel longitudinal profile, with downward and upward curvature leading to erosion and deposition, respectively (Mitchell 2006). Our simplified mathematical model is comparably similar to a transport-limited model because it allows for both erosion and deposition depending on the balance of $E_s v_s$ and $v_s(r_0 C)$ (Equation A7 in Appendix). However, as pointed out by Mitchell (2006), the dynamics of submarine gravity flows differ in a number of respects from river water (Peakall et al. 2000), which complicates the study of how submarine flow and seafloor morphology determine bed erosion rate and also the ability to discriminate between detachment-limited and transport-limited models from morphologic data. For example, the excess density of submarine flows relative to ambient seawater is much smaller than for river water and air, as a result, relatively minor changes in solid load arising from erosion or deposition can significantly alter flow velocity, leading to feedbacks with erosion (Parker et al. 1986; Mitchell 2006).

In summary, our analysis suggests that extrinsic characteristics of basin or continental-margin framework, sediment caliber and supply, and depositional-system age, and intrinsic sediment-gravity-flow dynamics significantly impact continental-margin relief and canyon-and-channel length (Fig. 5). Canyon-and-channel systems with short-lived, sand-rich sediment sources that form in relatively confined basins, some of which are subjected to rapid subsidence related to gravity-driven tectonic deformation, appear to develop distinctively different morphologies relative to longer-lived, finer-grained systems in large, unconfined ocean basins (Mutti and Normark 1987) (Fig. 5). The San Antonio (2), Kushiro (3), and Aoga (4) systems have much greater reliefs for their lengths relative to the other systems (Fig. 4A) as a result of their development across relatively steep, high-relief slopes that descend into deep trenches (e.g., Soh and Tokuyama 2002; Ranero et al. 2006; Noda et al. 2008; von Huene et al. 2009). The logarithmic relationship exhibited in Figure 4 (Equations 1 and 2) can be accounted for by the increased occurrence and magnitude of submarine mass wasting in higher-relief and correspondingly longer canyon-and-channel systems, limitations of relief imposed by the maximum depths of ocean basins, and sediment-gravity-flow dynamics (Fig. 5).

Applications to Subsurface and Outcrop Analogs

Mutti and Normark (1987) pioneered methods of relating seafloor observations to those of ancient subsurface and outcropping deep-water depositional systems for enhanced predictive models. They highlighted hierarchical common ground based on well-understood and thoroughly mapped systems, which could be used to predict tectono-stratigraphic characteristics such as type of basin, size of sediment source, physical and temporal scales, and stage of depositional-system development (Mutti and Normark 1987). A recent synthesis by Mutti et al. (2009) stresses that great caution should be exercised when comparing seafloor and ancient canyon-and-channel systems and depositional systems. In particular, different datasets, geologic contexts, scaling problems, and terminology cast doubt over the significance of such a comparison (Mutti et al. 2009). Despite the many problems encountered, the deep-water turbidite-system "element" approach, pioneered by Mutti and Normark (1987) and applied by Piper and Normark (2001), provides an easy, potentially meaningful descriptive tool to compare recent with ancient systems (Mutti et al. 2009). As indicated by our comparative quantitative morphologic analysis of seafloor canyon-and-channel systems, advances in submarine remote-sensing technology and improved deep-water depositional models allow for robust observations and potentially allow for the development of holistic stratigraphic models. That is, we document a nonlinear scaling relationship between continental-margin relief and canyon-and-channel system length that we interpret to have general predictive power (Equations 1 and 2). Our observations suggest that limited knowledge of the relief of an ancient basin margin, likened to the relief from a proximal canyon head to a distal channel terminus, can be employed in order to predict the basinward extent of a paleo–canyon-and-channel system and underlying depositional fan. Furthermore, the application also potentially works in reverse: intimate knowledge of the deep-water component of a basin or continental margin can facilitate understanding of other, up-depositional-dip stratigraphic architectures where data might be lacking.

As a test of these ideas and their applicability we measured the relief and length, from shelf edge across basin-floor fans, of 20 subsurface and outcropping paleo–shelf-slope–basin floor stratigraphic sequences (Table 2; Fig. 4B). Ideally, we would perform similar comparisons between modern and ancient canyon-and-channel systems. That is, we would measure the relief of an ancient basin margin in exactly the same way as the relief of a continental margin on the modern seafloor, from a proximal canyon head to a distal channel terminus. However, resolution limitations of subsurface seismic-stratigraphic sequences generally inhibit objective identification of canyon heads or channel termini (Normark et al. 1993). Similarly, outcropping stratigraphic sequences are inherently fragmentary and commonly do not exhibit the full expression of basin-margin canyon-and-channel systems (Normark et al. 1993).

The original depositional geometric form of the sequences is likely to have been different than the present-day form because of compaction of the sediment after deposition (Bahr et al. 2001; Deibert et al. 2003). Therefore, we applied a simple, order-of-magnitude decompaction correction (Angevine et al. 1990; p. 12):

$$T_O = [(1 - \Phi_N) T_N] / (1 - \Phi_O) \tag{4}$$

where T_O is the thickness of a sequence at the time of deposition, Φ_O is the original porosity at the time of deposition, and T_N and Φ_N are the present-day thickness and porosity of a sequence, respectively. The original and present-day porosities are universally assumed to be 0.50 and 0.25 for sandstone-dominated deep-sea depositional systems (cf. Deibert et al. 2003).

These stratigraphic sequences developed across ancient continental margins and in epicontinental seas and foreland basins (Table 2). Figure 4B shows a plot of seafloor canyon-and-channel systems and ancient subsurface and outcropping paleo–shelf-basin-floor sequences. There is a cluster of 12 subsurface and outcropping sequences that have an average decompacted relief of ~ 450 m, but range in length from 53 to 138 km (Table 2; gray diamonds in Fig. 4B). These sequences are from shallow epicontinental seas of the Western Siberian Basin, Western Interior Seaway, and Central Basin. These stratigraphic sequences reflect limited accommodation for vertical aggradation of depositional systems in relatively shallow epicontinental seas underlain by continental crust of normal thickness (e.g., the Cretaceous Western Siberian Basin, Russia; Pinous et al. 2001; the Cretaceous Western Interior Seaway, Wyoming; Carvajal and Steel 2006; the Eocene Central Basin, Spitsbergen; Helland-Hansen 1990, 1992; Plink-Björklund et al. 2001) (Fig. 7; gray diamonds in Fig. 4B). However, the range in length of these smaller-relief sequences indicates that appreciable sediment supply can significantly extend depositional systems across their shallow epicontinental seas (Carvajal et al. 2009).

The decompacted relief and length of eight other sequences generally fall within the range of seafloor canyon-and-channel systems. These sequences range in decompacted relief from ~ 900 to 2,600 m, and length from 13 to 217 km (Table 2; white diamonds in Fig. 4B). These sequences are predominantly from continental margins, however two sequences are from deep foreland basins, the Colville Trough and Magallanes Basin. Significant foreland-basin-margin relief was attained as a result of the combined effects of predecessor basin history (i.e., rifting and crustal stretching) and subsidence associated with collisional thrust loading, subduction dynamics, and foreland flexure (Fildani and Hessler 2005; Houseknecht et al. 2009; Romans et al. 2010; Romans et al. 2011). These margins had more accommodation for vertical aggradation of depositional systems and, as a result, grew to exhibit as much as an order of magnitude larger relief than the smaller epicontinental sequences (Fig. 7; white diamonds in Fig. 4B). Similar to the seafloor canyon-and-channel

TABLE 2.—*Ancient stratigraphic sequences and their paleo–basin-margin lengths and reliefs.*

Ancient stratigraphic sequences	Paleo-shelf edge-to-basin floor length (m)	Paleo-shelf edge-to-basin floor relief (m)	Decompacted relief (m)
(32) Porcupine sequence 2a	18300	610	915
(33) Main Pass (GOM) sequence A	142000	1390	2085
(34) Main Pass (GOM) sequence B	190000	1750	2625
(35) Main Pass (GOM) sequence C	210000	1720	2580
(36) Main Pass (GOM) sequence D	204000	1620	2430
(37) Main Pass (GOM) sequence E	217000	1520	2280
(38) Baltimore Canyon purple sequence	12600	410	615
(39) Neocomian Complex sequence S11	138000	330	495
(40) Neocomian Complex sequence S12	120000	380	570
(41) Neocomian Complex sequence S13	128000	370	555
(42) Lewis sequence C4	84000	280	420
(43) Lewis sequence C5	59000	280	420
(44) Lewis sequence C6	88000	300	450
(45) Lewis sequence C7	62000	330	495
(46) Battfjellet sequence 1	93000	350	525
(47) Battfjellet sequence 2	74000	280	420
(48) Battfjellet sequence 3	73000	260	390
(49) Battfjellet sequence 4	58000	230	345
(50) Battfjellet sequence 5	53000	200	300
(51) Tres Pasos Figueroa sequence	46000	870	1305

References: the Porcupine Basin, offshore western Ireland (Johannessen and Steel 2005); the Pliocene to Quaternary Main Pass area, Gulf of Mexico (He et al. 2006); the Miocene Baltimore Canyon region, offshore New Jersey (Poulsen et al. 1998); the Cretaceous Neocomian Complex, Western Siberian Basin, Russia (Pinous et al. 2001); the Cretaceous Lance–Fox Hills–Lewis shelf margin, Western Interior Seaway, Wyoming (Carvajal and Steel 2006); the Eocene Battfjellet Formation, Central Basin, Spitsbergen (Helland-Hansen 1990; Helland-Hansen 1992; Plink-Björklund et al. 2001); the Cretaceous Torok Formation, Colville Trough, North Slope, Alaska (McMillen 1991); the Cretaceous Tres Pasos Formation, Magallanes Basin, Chile (Hubbard et al. 2010).

examples, higher-relief ancient sequences are correspondingly longer (Fig. 7; white diamonds in Fig. 4B).

The sequence architectures documented herein reflect the accommodation and sediment-supply characteristics inherent to a given basin or continental-margin setting (cf. Jervey 1988). That is, the relief and length of sequences, where greatest, demonstrate relatively large accommodation and sediment supply. Similarly, the sequence architecture of relatively shallow epicontinental seas underlain by continental crust of normal thickness reflects limited accommodation and variable sediment supply.

Our analysis of examples of ancient stratigraphic sequences in the context of insights from seafloor canyon-and-channel systems demonstrates that knowledge of the relief of a shelf-to-basin-floor sequence, coupled with regional geologic information, including type of underlying crust and fluvio-deltaic sediment supply, can be used to predict the basinward extents of paleo–canyon-and-channel systems and associated depositional fans (Fig. 7). Our seafloor observations provide a nonlinear scaling relationship between continental-margin relief and canyon-and-channel-system length that has general predictive power (Equations 1 and 2). The decompacted relief and length of eight deep foreland basin and continental-margin sequences generally fall within the range of seafloor canyon-and-channel systems (Fig. 4B). The reasons for this correspondence are likely similar controls on relief-to-length relationships: intrinsic sediment-gravity-flow dynamics and more extrinsic characteristics of land-to-deep sea sediment supply and basin or continental-margin framework (Figs. 5, 7). Thus, regional geologic context of a frontier basin, including subsidence, accommodation, and sediment-supply characteristics, combined with scaling relationships documented herein, can provide predictions of the sizes of stratigraphic sequences. For example, sequences in a shallow foreland basin with active fold-and-thrust deformation might be $\sim$ 450 m thick but range in length from tens to $>$ 100 km depending on sediment supply. Likewise, limited knowledge of the relief of an ancient continental margin can be employed in order to predict the basinward extent of a paleo-canyon-and-channel system and underlying depositional fan (Figs. 4, 5, 7). Thus, the effective application of the insights documented herein hinges on integrating a basic

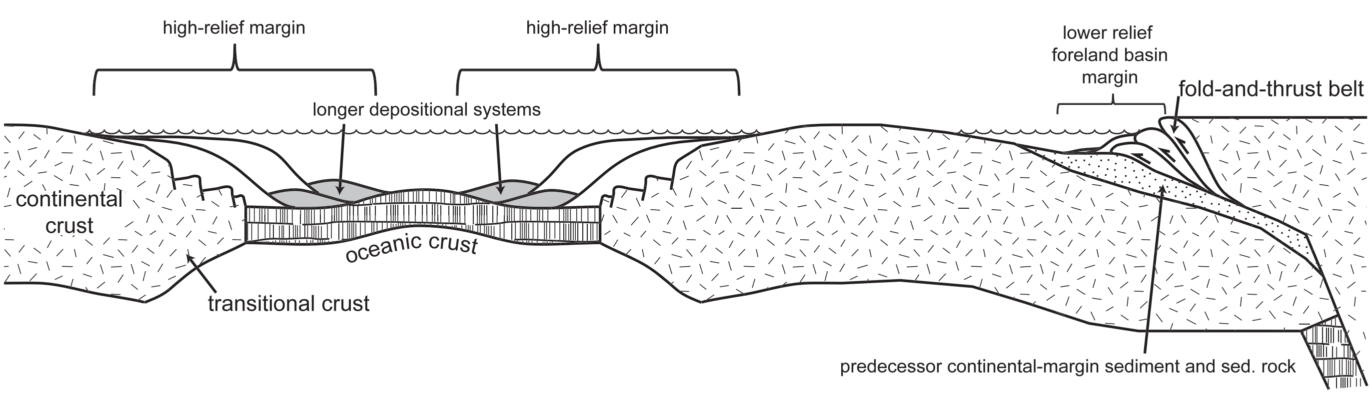

FIG. 7.—Stratigraphic-sequence development across continental margins and in a shallow foreland basin. Higher-relief continental margins exhibit as much as an order of magnitude larger relief and are longer than smaller foreland-basin sequences underlain by continental crust of normal thickness. Modified from Dickinson (1978).

understanding of regional geology with statistical relationships from analog seafloor and stratigraphic sequences.

Furthermore, the application potentially works in reverse: thoroughly mapped deep-water sedimentary systems can be employed to better understand regional geology. For example, the quantitative morphologic relationships documented herein also can be applied to up-dip staging areas. We interpret that nonlinearity in our observations of the seafloor can be partially accounted for by appreciable fluvio-deltaic sedimentation and consequent submarine mass wasting in higher-relief and correspondingly longer canyon-and-channel systems. Therefore, knowledge of the morphology (i.e., relief-to-length relationship) of a deep-water canyon-and-channel system or depositional fan can be used to predict the location along a depositional-system profile and character of the corresponding shallow-marine staging area and fluvio-deltaic sediment-dispersal system.

CONCLUSIONS

The longest canyon-and-channel systems of this study generally correspond with relatively mature, passive continental margins associated with some of the largest deep-sea fans in the world with long-term, voluminous, mud-rich sediment supply. These canyon-and-channel systems and their underlying depositional fans developed in relatively unconfined, open ocean basins and, as a result, grew to be relatively extensive. Shorter, lower-relief canyon-and-channel systems generally correspond with immature margins associated with relatively meager, sand-rich or mixed-caliber sediment supply. These systems generally form on continental-to-transitional crust where continuing tectonic activity resulted in relatively rapid changes in basin morphology and in short-lived sediment sources.

Seafloor continental-margin relief nonlinearly corresponds with canyon-and-channel-system length. We developed a scaling argument using a mathematical theory of a highly simplified sediment gravity flow that suggests flow dynamics are at least partially accountable for the nonlinearity. Measurements of outcropping and subsurface stratigraphic sequences from a range of basin settings corroborate observations of seafloor continental-margin canyon-and-channel systems: i.e., higher-relief ancient continental-margin and deep-foreland-basin sequences are correspondingly longer. But, a group of similarly low-relief sequences reflects the unique influence of the balance of accommodation and sediment supply on sequence architecture in epicontinental seas/foreland basins. Our compilation of seafloor canyon-and-channel systems and ancient stratigraphic sequences provides predictive insights into the development of submarine sediment-routing systems, which can be applied to natural-resource exploration in data-poor regions:

1. We document a nonlinear scaling relationship between continental-margin relief and canyon-and-channel system length (Equations 1 and 2) that can be directly employed to predict either of those morphologic parameters from knowledge of only one.
2. We demonstrate that regional tectono-stratigraphic context of a frontier basin, including subsidence, accommodation, and sediment supply, combined with the aforementioned scaling relationship can provide predictions of the morphologies of stratigraphic sequences.
3. We suggest that insights documented herein can potentially work in reverse: i.e., thoroughly mapped deep-water sedimentary systems can be employed to better understand the tectono-stratigraphic characteristics and up-depositional-dip stratigraphic architectures of a frontier basin.

ACKNOWLEDGMENTS

We thank the Clastic Stratigraphy R&D Team at Chevron Energy Technology Company and especially Julian Clark, Tim McHargue, and Henry Posamentier. We also thank George Hilley and the Stanford University Tectonic Geomorphology Laboratory. We recognize Bill Normark for invaluable discussions, insights, mentorship, and inspiration.

REFERENCES

Angevine, C.L., Heller, P.L., and Paola, C., 1990, Quantitative sedimentary basin modeling: American Association of Petroleum Geologists, Continuing Education Course Note Series, v. 32, 133 p.

Apps, G.M., Peel, F.J., Travis, C.J., and Yeilding, C.A., 1994, Structural controls on Tertiary deep-water deposition in the northern Gulf of Mexico, *in* Weimer, P., Bouma, A.H., and Perkins, B.F., eds., Submarine Fans and Turbidite Systems-Sequence Stratigraphy, Reservoir Architecture, and Production Characteristics, Gulf Coast Section, SEPM, 15th Annual Research Conference, p. 1–7.

Babonneau, N., Savoye, B., Cremer, M., and Klein, B., 2002, Morphology and architecture of the present canyon and channel system of the Zaire deep-sea fan: Marine and Petroleum Geology, v. 19, p. 445–467.

Bahr, D.B., Hutton, E.W.H., Syvitski, J.P.M., and Pratson, L.F., 2001, Exponential approximations to compacted sediment porosity profiles: Computers & Geosciences, v. 27, p. 691–700.

Barnes, N.E., and Normark, W.R., 1985, Diagnostic parameters for comparing modern submarine fans and ancient turbidite systems, *in* Bouma, A.H., Normark, W.R., and Barnes, N.E., eds., Submarine Fans and Related Turbidite Systems: New York, Springer-Verlag, p. 13–14.

Beaubouef, R.T., and Friedmann, S.J., 2000, High resolution seismic/sequence stratigraphic framework for the evolution of the Pleistocene intra slope basins, western Gulf of Mexico: depositional models and reservoir analogs, *in* Weimer, P., Slatt, R.M., Coleman, J., Rossen, N.C., Nelson, H., Bouma, A.H., Styzen, M.J., and Lawrence, D.T., eds., Deep-Water Reservoirs of the World, Gulf Coast Section, SEPM, 20th Annual Research Conference, Proceedings, p. 40–60.

Booth, J.R., DuVernay, A.E, III, Pfeiffer, D.S., and Styzen, M.J., 2000, Sequence stratigraphic framework, depositional models, and stacking patterns of ponded and slope fan systems in the Auger Basin: Central Gulf of Mexico slope, *in* Weimer, P., Slatt, R.M., Coleman, J., Rossen, N.C., Nelson, H., Bouma, A.H., Styzen, M.J., and Lawrence, D.T., eds., Deep-Water Reservoirs of the World, Gulf Coast Section, SEPM, 20th Annual Research Conference, Proceedings, p. 82–103.

Booth, J.S., O'Leary, D.W., Popenoe, P., and Danforth, W.W., 1993, U.S. Atlantic continental slope landslides; their distribution, general attributes, and implications: U.S. Geological Survey, Bulletin 2002, p. 14–22.

Bouma, A.H., Normark, W.R., and Barnes, N.E., 1985. Submarine Fans and Related Turbidite Systems: New York, Springer-Verlag, 351 p.

Brunner, C.A., Normark, W.R., Zuffa, G.G., and Serra, F., 1999, Deep-sea sedimentary record from the late Wisconsin cataclysmic floods from the Columbia River: Geology, v. 27, p. 463–466.

Burgess, P.M., and Hovius, N., 1998, Rates of delta progradation during highstands: consequences for timing of deposition in deep-marine systems: Geological Society of London, Journal, v. 15, p. 217–222.

Butman, B., Twichell, D.C., Rona, P.A., Tucholke, B.E., Middleton, T.J., and Robb, J.M., 2006, Sea floor topography and backscatter intensity of the Hudson Canyon region offshore of New York and New Jersey: U.S. Geological Survey, Open-File Report 2004-1441, http://pubs.usgs.gov/of/2004/1441/.

Carter, R.M., 1988, The nature and evolution of deep-sea channel systems: Basin Research, v. 1, p. 41–54.

Carvajal, C.R., and Steel, R.J., 2006, Thick turbidite successions from supply-dominated shelves during sea-level highstand: Geology, v. 34, p. 665–668.

Carvajal, C., Steel, R., and Petter, A., 2009, Sediment supply: the main driver of shelf-margin growth: Earth-Science Reviews, v. 96, p. 221–248.

Cleary, W.J., Pikley, O.H., and Nelson, J.C., 1985, Wilmington Fan, Atlantic Ocean, *in* Bouma, A.H., Normark, W.R., and Barnes, N.E., eds., Submarine Fans and Related Turbidite Systems: New York, Springer-Verlag, p. 157–164.

Clift, P.D., Hodges, K.V., Heslop, D., Hannigan, R., Van Long, H., and Calves, G., 2008, Correlation of Himalayan exhumation rates and Asian monsoon intensity: Nature Geoscience, v. 1, p. 875–880.

Collot, J.-Y., Agudelo, W., Ribodetti, A., and Marcaillou, B., 2008, Origin of a crustal splay fault and its relation to the seismogenic zone and underplating at the erosional north Ecuador–South Colombia oceanic margin: Journal of Geophysical Research, v. 113, B12102 p, doi: 10.1029/2008JB005691.

Covault, J.A., Fildani, A., Romans, B.W., and McHargue, T., 2011, The natural range of submarine canyon-and-channel longitudinal profiles: Geosphere, v. 7, p. 1–20.

Covault, J.A., Romans, B.W., Fildani, A., McGann, M., and Graham, S.A., 2010, Rapid climatic signal propagation from source to sink in a southern California sediment-routing system: The Journal of Geology, v. 118, p. 247–259.

Covault, J.A., and Romans, B.W., 2009, Growth patterns of deep-sea fans revisited: turbidite-system morphology in confined basins, examples from the California Borderland: Marine Geology, v. 265, p. 51–66.

Covault, J.A., Normark, W.R., Romans, B.W., and Graham, S.A., 2007, Highstand fans in the California borderland: the overlooked deep-water depositional systems: Geology, v. 35, p. 783–786.

Curray, J.R., Emmel, F.J., and Moore, D.G., 2002, The Bengal Fan: morphology, geometry, stratigraphy, history and processes: Marine and Petroleum Geology, v. 19, p. 1191–1223.

Damuth, J.E., 1994, Neogene gravity tectonics and depositional processes on the deep Niger Delta continental margin: Marine and Petroleum Geology, v. 11, p. 320–346.

Dartnell, P., Normark, W.R., Driscoll, N.W., Babcock, J.M., Gardner, J.V., Kvitek, R.G., and Iampietro, P.J., 2007, Multibeam Bathymetry and Selected Perspective Views Offshore San Diego, California: U.S. Geological Survey, Scientific Investigations, Map 2959, http://pubs.usgs.gov/sim/2007/2959/.

Deibert, J.E., Benda, T., Løseth, T., Schellpeper, M., and Steel, R.J., 2003, Eocene clinoform growth in front of a storm-wave-dominated shelf, Central Basin, Spitsbergen: no significant sand delivery to deepwater areas: Journal of Sedimentary Research, v. 73, p. 546–558.

Deptuck, M.E., Piper, D.J.W., Savoye, B., and Gervais, A., 2008, Dimensions and architecture of late Pleistocene submarine lobes off the northern margin of East Corsica: Sedimentology, v. 55, p. 869–898.

Dickinson, W.R., 1978, Plate tectonic evolution of sedimentary basins: American Association of Petroleum Geologists, Course Notes, v. 1, p. 1–56.

Divins, D.L., and Metzger, D., 2010, NGDC Coastal Relief Model: http://www.ngdc.noaa.gov/mgg/coastal/coastal.html.

Duncan, C.S., and Goff, J.A., 2001, Relict iceberg keel marks on the New Jersey outer shelf, southern Hudson Apron: Geology, v. 29, p. 411–414.

Fildani, A., and Hessler, A.M., 2005, Stratigraphic record across a retroarc basin inversion: Rocas Verdes–Magallanes Basin, Patagonian Andes, Chile: Geological Society of America, Bulletin, v. 117, p. 1596–1614.

Fildani, A., and Normark, W.R., 2004, Late Quaternary evolution of channel and lobe complexes of Monterey Fan: Marine Geology, v. 206, p. 199–213.

Flood, R.D., and Damuth, J.E., 1987, Quantitative characteristics of sinuous distributary channels on the Amazon deep-sea fan: Geological Society of America, Bulletin, v. 98, p. 728–738.

Flood, R.D., Manley, P.L., Kowsmann, R.O., Appi, C.J., and Pirmez, C., 1991, Seismic facies and late Quaternary growth of Amazon submarine fan, *in* Weimer, P., and Link, M.H., eds., Seismic Facies and Sedimentary Processes of Submarine Fans and Turbidite Systems: New York, Springer-Verlag, p. 415–433.

Fukushima, Y., Parker, G., and Pantin, H.M., 1985, Prediction of ignitive turbidity currents in Scripps Submarine Canyon: Marine Geology, v. 67, p. 55–81.

Fulthorpe, C.S., and Austin, J.A, Jr, 2004, Shallowly buried, enigmatic seismic stratigraphy on the New Jersey mid-outer shelf: evidence for latest Pleistocene catastrophic erosion?: Geology, v. 32, p. 1013–1016.

Garcia, M., and Parker, G., 1991, Entrainment of bed sediment into suspension: Journal of Hydraulic Engineering, v. 117, p. 414–435.

Gardner, J.V., and Dartnell, P., 2002, Multibeam mapping of the Los Angeles, California margin: U.S. Geological Survey, Open-File Report 02-162, http://geopubs.wr.usgs.gov/open-file/of02-162/.

Gerber, T.P., Amblas, D., Wolinsky, M.A., Pratson, L.F., and Canals, M., 2009, A model for the long-profile shape of submarine canyons: Journal of Geophysical Research, v. 114, F03002 p, doi: 10.1029/2008JF001190.

Gorsline, D.S., and Emery, K.O., 1959, Turbidity-current deposits in San Pedro and Santa Monica basins off southern California: Geological Society of America, Bulletin, v. 70, p. 279–290.

Graham, S.A., and Bachman, S.B., 1983, Structural controls on submarine-fan geometry and internal architecture: upper La Jolla fan system, offshore southern California: American Association of Petroleum Geologists, Bulletin, v. 67, p. 83–96.

Greene, H.G., Maher, N.M., and Paull, C.K., 2002, Physiography of the Monterey Bay National Marine Sanctuary and implications about continental margin development: Marine Geology, v. 181, p. 55–82.

Greenlee, S.M., Devlin, W.J., Miller, K.G., Mountain, G.S., and Flemings, P.B., 1992, Integrated sequence stratigraphy of Neogene deposits, New Jersey continental shelf and slope: comparison with the Exxon model: Geological Society of America, Bulletin, v. 104, p. 1403–1411.

He, L., Dawers, N., and Stelting, C., 2006, Post 30 m.y. sequence stratigraphy, northeastern Gulf of Mexico: American Association of Petroleum Geologists, Search and Discovery article #30045, http://www.searchanddiscovery.net/documents/2006/06129he/index.htm.

Helland-Hansen, W., 1990, Sedimentation in Paleogene foreland basin, Spitsbergen: American Association of Petroleum Geologists, Bulletin, v. 74, p. 260–272.

Helland-Hansen, W., 1992, Geometry and facies of Tertiary clinothems, Spitsbergen: Sedimentology, v. 39, p. 1013–1029.

Houseknecht, D.W., Bird, K.J., and Schenk, C.J., 2009, Seismic analysis of clinoform depositional sequences and shelf-margin trajectories in Lower Cretaceous (Albian) strata, Alaska North Slope: Basin Research, v. 21, p. 644–654.

Howard, A.D., 1994, A detachment-limited model of drainage basin evolution: Water Resources Research, v. 30, p. 2261–2285.

Hubbard, S.M., Fildani, A., Romans, B.W., Covault, J.A., and McHargue, T.R., 2010, High-relief slope clinoform development: insights from outcrop, Magallanes Basin, Chile: Journal of Sedimentary Research, v. 80, p. 357–375.

Huyghe, P., Foata, M., Deville, Mascle, G., Caramba Working Group (2004), Channel profiles through the active thrust front of the southern Barbados prism: Geology, v. 32, p. 429–432.

Inman, D.L., 2008. Highstand fans in the California borderland: comment: Geology, Online Forum, e166 p.

Inman, D.L., and Jenkins, S.A., 1999, Climate change and the episodicity of sediment flux of small California rivers: The Journal of Geology, v. 107, p. 251–270.

Jegou, I., Savoye, B., Pirmez, C., and Droz, L., 2008, Channel-mouth lobe complex of the recent Amazon Fan: the missing piece: Marine Geology, v. 252, p. 62–77.

Jervey, M.T., 1988, Quantitative geological modeling of siliciclastic rock sequences and their seismic expression, *in* Wilgus, C.K., Hastings, B.S., Posamentier, H., Van Wagoner, J., Ross, C.A., and Kendall, C.G.St.C., eds., Sea-Level Changes: An Integrated Approach, SEPM, Special Publication 42, p. 47–70.

Johannessen, E., and Steel, R., 2005, Shelf-margin clinoforms and prediction of deepwater sands: Basin Research, v. 17, p. 521–550.

Klaus, A., and Taylor, B., 1991, Submarine canyon development in the Izu-Bonin forearc: A SeaMARC II and seismic survey of Aoga Shima Canyon: Marine Geophysical Researches, v. 13, p. 131–152.

Knudson, K.P., and Hendy, I.L., 2009, Climatic influences on sediment deposition and turbidite frequency in the Nitinat Fan, British Columbia: Marine Geology, v. 262, p. 29–38.

Kolla, V., and Coumes, F., 1987, Morphology, internal structure, seismic stratigraphy, and sedimentation of Indus Fan: American Association of Petroleum Geologists, Bulletin, v. 71, p. 650–677.

Kolla, V., and Macurda, D., 1988, Sea-level changes and timing of turbidity-current events in deep-sea fan systems, *in* Wilgus, C.K., Hastings, B.S., Posamentier, H., Van Wagoner, J., Ross, C.A., and Kendall, C.G.St.C., eds., Sea-Level Changes: An Integrated Approach, SEPM, Special Publication 42, p. 381–392.

Lambeck, K., and Chappell, J., 2001, Sea level change through the last glacial cycle: Science, v. 292, p. 679–686.

Laursen, J., and Normark, W.R., 2002, Late Quaternary evolution of the San Antonio Submarine Canyon in the Central Chile forearc (~ 33°S): Marine Geology, v. 188, p. 365–390.

Mallarino, G., Beaubouef, R.T., Droxler, A.W., Abreu, V., and Labeyrie, L., 2006, Sea level influence on the nature and timing of a minibasin sedimentary fill (northwestern slope of the Gulf of Mexico): American Association of Petroleum Geologists, Bulletin, v. 90, p. 1089–1119.

McAdoo, B.G., Pratson, L.F., and Orange, D.L., 2000, Submarine landslide geomorphology, US continental slope: Marine Geology, v. 169, p. 103–136.

Melnick, D., Bookhagen, B., Echtler, H.P., and Strecker, M.R., 2006, Coastal deformation and great subduction earthquakes, Isla Santa María, Chile (37°S): Geological Society of America, Bulletin, v. 118, p. 1463–1480.

Menard, H.W., 1955, Deep-sea channels, topography, and sedimentation: American Association of Petroleum Geologists, Bulletin, v. 39, p. 236–255.

McMillen, K.M., 1991, Seismic stratigraphy of Lower Cretaceous foreland basin submarine fans in the North Slope, Alaska, *in* Weimer, P., and Link, M.H., eds., Seismic Facies and Sedimentary Processes of Submarine Fans and Turbidite Systems: New York, Springer-Verlag, p. 289–302.

Milliman, J.D., and Syvitski, J.P.M., 1992, Geomorphic/tectonic control of sediment discharge to the ocean; the importance of small mountainous rivers: The Journal of Geology, v. 100, p. 525–544.

Milliman, J.D., Rutkowski, C., and Meybeck, M., 1995, River Discharge to the Sea: A Global River Index (GLORI): Land–Ocean Interactions in the Coastal Zone, Reports and Studies 34, 125 p.

Mitchell, N.C., 2006, Morphologies of knickpoints in submarine canyons: Geological Society of America, Bulletin, v. 118, p. 589–605.

Mutti, E., 1992, Turbidite Sandstones: Instituto di Geologia Università di Parma, Agip S.P.A., 275 p.

Mutti, E., and Normark, W.R., 1987, Comparing examples of modern and ancient turbidite systems: problems and concepts, *in* Leggett, J.K., and Zuffa, G.G., eds., Marine Clastic Sedimentology: Concepts and Case Studies: London, Graham & Trotman, p. 1–38.

Mutti, E., and Normark, W.R., 1991, An integrated approach to the study of turbidite systems, *in* Weimer, P., and Link, M.H., eds., Seismic Facies and Sedimentary Processes of Submarine Fans and Turbidite Systems: New York, Springer-Verlag, p. 75–106.

Mutti, E., Bernoulli, D., Ricci Lucchi, F., and Tinterri, R., 2009, Turbidites and turbidity currents from Alpine "flysch" to the exploration of continental margins: Sedimentology, v. 56, p. 267–318.

Nelson, C.H., and Kulm, L.D., 1973, Submarine fans and channels, *in* Middleton, G.V., and Bouma, A.H., eds., Turbidites and Deep Water Sedimentation, SEPM, Short Course Notes, p. 39–70.

Nelson, C.H., Carlson, P.R., Byrne, J.V., and Alpha, T.R., 1970, Development of the Astoria Canyon–Fan physiography and comparison with similar systems: Marine Geology, v. 8, p. 259–291.

Nelson, C.H., Maldonado, A., Coumes, F., Got, H., and Monaco, A., 1985, Ebro Fan, Mediterranean, *in* Bouma, A.H., Normark, W.R., and Barnes, N.E., eds., Submarine Fans and Related Turbidite Systems: New York, Springer-Verlag, p. 121–128.

Nilsen, T.H., 1980, Modern and ancient submarine fans: discussion of papers by R.G. Walker and W.R. Normark: American Association of Petroleum Geologists, Bulletin, v. 64, p. 1094–1101.

Noda, A., Tuzino, T., Furukawa, R., Joshima, M., and Uchida, J., 2008, Physiographical and sedimentological characteristics of submarine canyons developed upon an active forearc slope: The Kushiro submarine canyon, northern Japan: Geological Society of America, Bulletin, v. 120, p. 750–767.

Normark, W.R., 1970, Growth patterns of deep-sea fans: American Association of Petroleum Geologists, Bulletin, v. 54, p. 2170–2195.

Normark, W.R., 1978, Fan valleys, channels, and depositional lobes on modern submarine fans; characters for recognition of sandy turbidite environments: American Association of Petroleum Geologists, Bulletin, v. 62, p. 912–931.

Normark, W.R., 1985, Local morphologic controls and effects of basin geometry on flow processes in deep marine basins, *in* Zuffa, G.G., ed., Provenance of Arenites, North Atlantic Treaty Organization, Advanced Science Institutes Series C-148, p. 47–63.

Normark, W.R., and Gutmacher, C.E., 1985, Delgada Fan, Pacific Ocean, *in* Bouma, A.H., Normark, W.R., and Barnes, N.E., eds., Submarine Fans and Related Turbidite Systems: New York, Springer-Verlag, p. 59–64.

Normark, W.R., and Piper, D.J.W., 1985, Navy Fan, Pacific Ocean, *in* Bouma, A.H., Normark, W.R., and Barnes, N.E., eds., Submarine Fans and Related Turbidite Systems: New York, Springer-Verlag, p. 87–94.

Normark, W.R., Piper, D.J.W., and Hess, G.R., 1979, Distributary channels, sand lobes, and mesotopography of Navy submarine fan, California borderland, with applications to ancient fan sediments: Sedimentology, v. 26, p. 749–774.

Normark, W.R., Gutmacher, C.E., Chase, T.E., and Wilde, P., 1985, Monterey Fan, Pacific Ocean, *in* Bouma, A.H., Normark, W.R., and Barnes, N.E., eds., Submarine Fans and Related Turbidite Systems: New York, Springer-Verlag, p. 79–86.

Normark, W.R., Posamentier, H., and Mutti, E., 1993, Turbidite systems: state of the art and future directions: Reviews of Geophysics, v. 31, p. 91–116.

Normark, W.R., Piper, D.J.W., and Sliter, R., 2006, Sea-level and tectonic control of middle to late Pleistocene turbidite systems in Santa Monica Basin, offshore California: Sedimentology, v. 53, p. 867–897.

Normark, W.R., Piper, D.J.W., Romans, B.W., Covault, J.A., and Dartnell, P., 2009, Submarine canyon and fan systems of the California Continental Borderland, *in* Lee, H., and Normark, W.R., eds., Earth Science in the Urban Ocean: the Southern California Continental Borderland, Geological Society of America, Special Paper 454, p. 141–168.

Parker, G., Fukushima, Y., and Pantin, H.M., 1986, Self-accelerating turbidity currents: Journal of Fluid Mechanics, v. 171, p. 619–628.

Parker, G., Garcia, M.H., Fukushima, Y., and Yu, W., 1987, Experiments on turbidity currents over an erodible bed: Journal of Hydraulic Research, v. 25, p. 123–147.

Payton, C.E., 1977, Seismic Stratigraphy—Applications to Hydrocarbon Exploration: American Association of Petroleum Geologists, Memoir 26, 516 p.

Peakall, J., McCaffrey, W., and Kneller, B., 2000, A process model for the evolution, morphology, and architecture of sinuous submarine channels: Journal of Sedimentary Research, v. 70, p. 434–448.

Pickering, K.T., 1982, The shape of deep-water siliciclastic systems: a discussion: Geo-Marine Letters, v. 2, p. 41–46.

Pinous, O.V., Levchuk, M.A., and Sahagian, D.L., 2001, Regional synthesis of the productive Neocomian complex of West Siberia: sequence stratigraphic framework: American Association of Petroleum Geologists, Bulletin, v. 85, p. 1713–1730.

Piper, D.J.W., and Normark, W.R., 2001, Sandy fans-from Amazon to Hueneme and beyond: American Association of Petroleum Geologists, Bulletin, v. 85, p. 1407–1438.

Piper, D.J.W., and Normark, W.R., 2009, Processes that initiate turbidity currents and their influence on turbidites: a marine geology perspective: Journal of Sedimentary Research, v. 79, p. 347–362.

Piper, D.J.W., Shaw, J., and Skene, K.I., 2007, Stratigraphic and sedimentological evidence for late Wisconsinan subglacial outburst floods to Laurentian Fan: Palaeogeography, Palaeoclimatology, Palaeoecology, v. 246, p. 101–119.

Pirmez, C., and Imran, J., 2003, Reconstruction of turbidity currents in Amazon Channel: Marine and Petroleum Geology, v. 20, p. 823–849.

Pirmez, C., Beaubouef, R.T., Friedmann, S.J., and Mohrig, D.C., 2000, Equilibrium profile and baselevel in submarine channels: examples from late Pleistocene systems and implications for the architecture of deepwater reservoirs, *in* Weimer, P., Slatt, R.M., Coleman, J., Rossen, N.C., Nelson, H., Bouma, A.H., Styzen, M.J., and Lawrence, D.T., eds., Deep-Water Reservoirs of the World, Gulf Coast Section, SEPM, 20th Annual Research Conference, Proceedings, p. 782–805.

Plink-Björklund, P., Mellere, D., and Steel, R.J., 2001, Turbidite variability and architecture of sand-prone, deep-water slopes; Eocene clinoforms in the Central Basin, Spitsbergen: Journal of Sedimentary Research, v. 71, p. 895–912.

Posamentier, H.W., and Kolla, V., 2003, Seismic geomorphology and stratigraphy of depositional elements in deep-water settings: Journal of Sedimentary Research, v. 73, p. 367–388.

Posamentier, H.W., Erskine, R.D., and Mitchum, R.M., 1991, Models for submarine-fan deposition within a sequence-stratigraphic framework, *in* Weimer, P., and Link, M.H., eds., Seismic Facies and Sedimentary Processes of Submarine Fans and Turbidite Systems: New York, Springer-Verlag, p. 127–136.

Poulsen, C.J., Flemings, P.B., Robinson, R.A.J., and Metzger, J.M., 1998, Three-dimensional stratigraphic evolution of the Miocene Baltimore Canyon region: implications for eustatic interpretations and the systems tract model: Geological Society of America, Bulletin, v. 110, p. 1105–1122.

Prather, B.E., Booth, J.R., Steffens, G.S., and Craig, P.A., 1998, Classification, lithologic calibration, and stratigraphic succession of seismic facies of intraslope basins, deep water Gulf of Mexico: American Association of Petroleum Geologists, Bulletin, v. 82, p. 701–728.

Pratson, L.F., and Haxby, W.F., 1996, What is the slope of the U.S. continental slope?: Geology, v. 24, p. 3–6.

Pratson, L.F., and Ryan, W.B.F., 1994, Pliocene to Recent infilling and subsidence of intraslope basins offshore Louisiana: American Association of Petroleum Geologists, Bulletin, v. 78, p. 1483–1506.

Pratson, L.F., Ryan, W.B.F., Mountain, G.S., and Twichell, D.C., 1994, Submarine canyon initiation by downslope-eroding sediment flows: evidence in late Cenozoic strata on the New Jersey continental slope: Geological Society of America, Bulletin, v. 106, p. 395–412.

Ranero, C.R., von Huene, R., Weinrebe, W., and Reichert, C., 2006, Tectonic processes along the Chile convergent margin, *in* Oncken, O., Chong, G., and Franz, G., eds., The Andes: Active Subduction Orogeny: Berlin, Springer-Verlag, p. 91–121.

Reading, H.G., and Richards, M., 1994, Turbidite systems in deep-water basin margins classified by grain size and feeder system: American Association of Petroleum Geologists, Bulletin, v. 78, p. 792–822.

Romans, B.W., Normark, W.R., McGann, M.M., Covault, J.A., and Graham, S.A., 2009, Coarse-grained sediment delivery and distribution in the Holocene Santa Monica Basin, California; implications for evaluating source-to-sink flux at millennial time scales: Geological Society of America, Bulletin, v. 121, p. 1394–1408.

Romans, B.W., Fildani, A., Graham, S.A., Hubbard, S.M., and Covault, J.A., 2010, Importance of predecessor basin history on the sedimentary fill of a retroarc foreland basin: provenance analysis of the Cretaceous Magallanes basin, Chile (50–52°S): Basin Research, v. 22, p. 640–658.

Romans, B.W., Fildani, A., Hubbard, S.M., Covault, J.A., Fosdick, J.C., and Graham, S.A., 2011, Evolution of deep-water stratigraphic architecture, Magallanes Basin, Chile: Marine and Petroleum Geology, v. 28, p. 612–628.

Rowan, M.G., Peel, F.J., and Vendeville, B.C., 2004, Gravity-driven fold belts on passive margins, *in* McClay, K.R., ed., Thrust Tectonics and Hydrocarbon Systems, American Association of Petroleum Geologists, Memoir 82, p. 157–182.

Ryan, W.B.F., Carbotte, S.M., Coplan, J.O., O'Hara, S., Melkonian, A., Arko, R., Weissel, R.A., Ferrini, V., Goodwillie, A., Nitsche, F., Bonczkowski, J., and Zemsky, R., 2009, Global multi-resolution topography synthesis: Geochemistry Geophysics Geosystems, v. 10, Q03014 p, doi: 10.1029/2008GC002332.

Savoye, B., Piper, D.J.W., and Droz, L., 1993, Plio-Pleistocene evolution of the Var deep-sea fan off the French Riviera: Marine and Petroleum Geology, v. 10, p. 550–571.

Schlee, J.S., and Robb, J.M., 1991, Submarine processes of the middle Atlantic continental rise based on GLORIA imagery: Geological Society of America, Bulletin, v. 103, p. 1090–1103.

Shanmugam, G., and Moiola, R.J., 1988, Submarine fans: characteristics, models, classification, and reservoir potential: Earth-Science Reviews, v. 24, p. 383–428.

Shepard, F.P., 1948. Submarine Geology: New York, Harper and Brothers, 338 p.

Skene, K.I., and Piper, D.J.W., 2006, Late Cenozoic evolution of Laurentian Fan; development of a glacially-fed submarine fan: Marine Geology, v. 217, p. 67–92.

Soh, W., and Tokuyama, H., 2002, Rejuvenation of submarine canyon associated with ridge subduction, Tenryu Canyon, off Tokai, central Japan: Marine Geology, v. 187, p. 203–220.

Sømme, T.O., Helland-Hansen, W., Martinsen, O.J., and Thurmond, J.B., 2009a, Relationship between morphological and sedimentological parameters in source-to-sink systems; a basis for predicting semi-quantitative characteristics in subsurface systems: Basin Research, v. 21, p. 361–387.

Sømme, T.O., Martinsen, O.J., and Thurmond, J.B., 2009b, Reconstructing morphological and depositional characteristics in subsurface sedimentary systems; an example from the Maastrichtian–Danian Ormen Lange system, More Bain, Norwegian Sea: American Association of Petroleum Geologists, Bulletin, v. 93, p. 1347–1377.

Sømme, T.O., Piper, D.J.W., Deptuck, M.E., and Helland-Hansen, W., 2011, Linking onshore–offshore sediment dispersal in the Golo source-to-sink system (Corsica, France) during the Late Quaternary: Journal of Sedimentary Research, v. 81, p. 118–137.

Steffens, G.S., Biegert, E.K., Sumner, H.S., and Bird, D., 2003, Quantitative bathymetric analyses of selected deepwater siliciclastic margins; receiving basin configurations for deepwater fan systems: Marine and Petroleum Geology, v. 20, p. 529–545.

Stow, D.A.V., Howell, D.G., and Nelson, C.H., 1985, Sedimentary, tectonic, and sea-level controls, *in* Bouma, A.H., Normark, W.R., and Barnes, N.E., eds., Submarine Fans and Related Turbidite Systems: New York, Springer-Verlag, p. 15–22.

Traer, M.M., Hilley, G.E., Fildani, A., and McHargue, T., in press, The sensitivity of turbidity currents to mass and momentum exchanges between these underflows and their surroundings: Journal of Geophysical Research.

Tucker, G.E., and Whipple, K.X., 2002, Topographic outcomes predicted by stream erosion models: sensitivity analysis and intermodel comparison: Journal of Geophysical Research, v. 107, 2179 p, doi: 10.1029/2001JB000162.

Twichell, D.C., Nelson, C.H., Damuth, J.E., and Dunhill, G., 2000, Bryant Canyon turbidite system pathway on the Louisiana continental slope, *in* Weimer, P., Slatt, R.M., Coleman, J., Rosen, N.C., Nelson, C.H., Bouma, A.H., Styzen, M.J., and Lawrence, D.T., eds., Deep-Water Reservoirs of the World, Gulf Coast Section, SEPM, 20th Annual Research Conference, p. 1032–1044.

Underwood, M.B., Hoke, K.D., Fisher, A.T., Davis, E.E., Giamalvo, E., Zühlsdorff, L., and Spinelli, G.A., 2005, Provenance, stratigraphic architecture, and hydrogeologic influence of turbidites on the Mid-Ocean Ridge flank of northwestern Cascadia Basin, Pacific Ocean: Journal of Sedimentary Research, v. 75, p. 149–164.

von Huene, R., Ranero, C.R., and Scholl, D.W., 2009, Convergent margin structure in high-quality geophysical images and current kinematic and dynamic models, *in* Lallemand, S., and Funiciello, F., eds., Subduction Zone Geodynamics: Berlin, Springer-Verlag, p. 137–157.

Walker, R.G., 1978, Deep-water sandstone facies and ancient submarine fans; models for exploration for stratigraphic traps: American Association of Petroleum Geologists, Bulletin, v. 62, p. 932–966.

Wetzel, A., 1993, The transfer of river load to deep-sea fans: a quantitative approach: American Association of Petroleum Geologists, Bulletin, v. 77, p. 1679–1692.

Wilgus, C.K., Hastings, B.S., Posamentier, H., Van Wagoner, J., Ross, C.A., and Kendall, C.G.St.C., eds., Sea-Level Changes: An Integrated Approach: SEPM, Special Publication 42, 407 p.

Wynn, R.B., Kenyon, N.H., Masson, D.G., Stow, D.A.V., and Weaver, P.P.E., 2002, Characterization and recognition of deep-water channel-lobe transition zones: American Association of Petroleum Geologists, Bulletin, v. 86, p. 1441–1462.

Zuffa, G.G., Normark, W.R., Serra, F., and Brunner, C.A., 2000, Turbidite megabeds in an oceanic rift valley recording Jökulhlaups of late Pleistocene glacial lakes of the western United States: The Journal of Geology, v. 108, p. 253–274.

Received 20 July 2010; accepted 1 September 2011.

APPENDIX

The following is not intended as a complete description of the dynamics of a turbidity current. Rather, it is presented to illustrate that turbidity currents and their flow dynamics, even in a grossly over-simplified form, will behave nonlinearly, and that this nonlinearity affects the margin relief/run-out distance relationship. Assuming a steady, uniform flow, the momentum budget for a turbidity current may be written as (e.g., Parker et al. 1986):

$$Uh(\partial U/\partial x) = RgChS - (1/2)Rg\left(\partial Ch^2/\partial x\right) - u*^2 - e_W U^2 \qquad \text{(A1)}$$

where the flow dynamics of interest are velocity (U), height (h), and concentration (C). Other variables include the coefficient of clear-water entrainment (e_w) (Parker et al. 1986; Parker et al. 1987), the slope traversed by the flow (S), the submerged specific gravity of sediment (R), and gravitational acceleration (g). The bed shear velocity ($u*$) can be described by (Parker et al. 1986):

$$u*^2 = c_D U^2 \qquad \text{(A2)}$$

or

$$u*^2 = aK \qquad \text{(A3)}$$

where c_D is the coefficient of bed roughness, α is a turbulence scaling parameter roughly equal to 0.1, and K is the mean turbulent kinetic energy per unit mass that co-varies with the other flow dynamics (see Parker et al. 1986). The change in formulae results from consideration of an additional energy balance to describe the flow dynamics of a turbidity current (see Parker et al. 1986). For simplicity, we will use Equation A1 herein to describe the bed-shear velocity.

Analysis of Equation A1 shows that flow velocity, directly related to run-out distance, behaves in a nonlinear fashion. However, it remains unclear how this nonlinearity relates to the ratio of margin relief to run-out distance. To best illustrate this, we make another significant assumption that down-stream changes in flow concentration and flow height (second term on the RHS of Equation A1) are negligible compared to the driving force of gravity (first term on the RHS of Equation A1) and the frictional forces (third and fourth terms on the RHS of Equation A1). This assumption does not arise from any motivation other than attempting to describe the simplest turbidity current; one in which the driving force is entirely balanced by frictional forces. From this assumption in addition to uniform, steady flow:

$$RghCS = (c_D + e_W)U^2 \qquad \text{(A4)}$$

The clear-water entrainment rate is typically cast in terms of the flow dynamics via the flow Richardson's number:

$$Ri = RghC/U^2 \qquad \text{(A5)}$$

Isolating slope from Equation A4:

$$\mathrm{S} = \left[(c_D + e_W)U^2\right]/(RghC) \qquad \text{(A6)}$$

In this simplified model, slope can be viewed as an average canyon-and-channel slope defined by the margin relief and canyon-and-channel run-out distance. Because the excess density of sediment is fundamentally important in propelling gravity flows basinward, and concentration varies co-dependently with velocity, it is helpful to find an expression for concentration (C) in terms of the flow velocity. The net volume rate of entrainment of sediment into suspension per unit bed area per unit time is described by $v_s(E_s - r_0C)$, where v_s is sediment fall velocity, r_0 is the ratio of near-bed to depth-averaged concentration, and E_s is the dimensionless sediment entrainment rate (Fukushima et al. 1985; Parker et al. 1986). Thus, for steady, uniform flow at the erosional-to-depositional transition:

$$v_s(r_0 C) = E_s v_s \qquad \text{(A7)}$$

$$C = E_s/r_0 \qquad \text{(A8)}$$

Using a simplified form of the sediment entrainment rate developed by Garcia and Parker (1991):

$$E_s = FZ_u{}^5 \qquad \text{(A9)}$$

where F is a constant and Z_u is described by:

$$Z_u = \left(c_D{}^{1/2}U/v_s\right)R_p{}^{0.6} \qquad \text{(A10)}$$

with the particle Reynold's number (R_p) being:

$$R_p = \left[(RgD_s)^{1/2}D_s\right]/v \qquad \text{(A11)}$$

where D_s is the sediment grain diameter and v is the kinematic viscosity of water. Substituting (A9) into (A8) and expanding with (A10):

$$C = (F/r_0)\left(c_D{}^{5/2}/v_s{}^5\right)R_p{}^3U^5 \qquad \text{(A12)}$$

Finally, substitution of (A12) into (A6) yields Equation (3).